



Assessment and health effects of radon and its relation with some parameters in groundwater sources from shallow aquifers in granitic terrains, southeastern axis of Ibadan, Nigeria

Theophilus Aanuoluwa Adagunodo^{a,*}, Abraham Adewale Aremu^b, Oyelowo Gabriel Bayowa^c, Ayobami Ismaila Ojoawo^d, Abosede Olufunmi Adewoye^c, Temiloluwa Ezekiel Olonade^a

^a Department of Physics, Covenant University, Ota, Ogun State, Nigeria

^b Department of Pure and Applied Physics, Ladake Akintola University of Technology, Ogbomoso, Oyo State, Nigeria

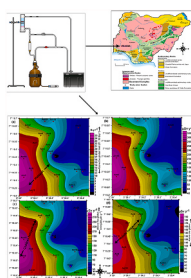
^c Department of Earth Sciences, Ladake Akintola University of Technology, Ogbomoso, Oyo State, Nigeria

^d Department of Physics, University of Ibadan, Ibadan, Oyo State, Nigeria

HIGHLIGHTS

- Radon concentrations in groundwater sources and health effects within crystalline basement rocks were assessed.
- Effect of dumpsite on radon concentrations in crystalline aquifers was determined statistically.
- Variations of radon concentrations and its health effects on all the age groups increased along the fault lines.
- It was revealed that the radon pathway to the aquifer system is mainly through the geogenic contribution.

GRAPHICAL ABSTRACT



ARTICLE INFO

Keywords:

Groundwater
Radon
Aquifer
Thoron
Crystalline basement complex
Faults

ABSTRACT

Assessing the level of radon concentrations in water for domestic purposes is important because it will reveal if the consumption and uses of such water is safe. This study was conceived with the aim to ascertain the integrity of water being consumed and used for other activities as well as to determine the source of radon concentrations in shallow aquifers within the granitic rocks of Amuloko and Olorunsogo areas in Ibadan, Nigeria. Concentrations and health effects of radon in 40 groundwater samples were analyzed using RAD7 detector. In Amuloko area, the radon concentrations and the total annual effective dose received in groundwater varied from 3.00 to 24.50 Bq l⁻¹ and 29.49 to 240.61 μSv y⁻¹. The mean and the standard deviation (SD) of radon concentrations and the total annual effective doses received in groundwater by adults in Amuloko area are 13.45 ± 6.58 Bq l⁻¹ and 132.06 ± 64.62 μSv y⁻¹. In Olorunsogo (control points), the radon concentrations and the total annual effective dose received in groundwater varied from 3.18 to 20.00 Bq l⁻¹ and 31.18 to 196.42 μSv y⁻¹. The mean and the SD of radon concentrations and the total annual effective doses received in groundwater by adults at the control points are 12.06 ± 4.74 Bq l⁻¹ and 118.47 ± 46.57 μSv y⁻¹, in sequence. The mean radon concentrations and the mean total annual effective dose received in groundwater were higher than the threshold limits of 11.10 Bq l⁻¹ and 100.00 μSv y⁻¹ by factors of 1.21 and 1.32 (in Amuloko), and 1.09 and 1.19 (in Olorunsogo), respectively. It is established that no significant variation exists between the sources of radon concentrations in the shallow

* Corresponding author.

E-mail addresses: taadagunodo@yahoo.com, theophilus.adagunodo@covenantuniversity.edu.ng (T.A. Adagunodo).

<https://doi.org/10.1016/j.gsd.2023.100930>

Received 24 October 2022; Received in revised form 31 January 2023; Accepted 21 February 2023

Available online 25 February 2023

2352-801X/© 2023 Elsevier B.V. All rights reserved.

aquifers from the two settlements. This suggests that the elevated concentrations of radon at the two settlements are due to the geological contributions of faults.

1. Introduction

About 70% of the Earth's surface is covered with water. Water being an easy solvent, enables most pollutants to dissolve in it and gets contaminated (Saeed and Hassan, 2015). The quality of this vital resource could be deteriorated due to anthropogenic activities. Groundwater is often cheaper, more convenient and less vulnerable to pollution than surface water. Therefore it is commonly used for public water supplies. The rate at which groundwater is being polluted is lesser than that of surface water. When groundwater is polluted, it is not easily cleaned up. Waste disposal and management remains one of the major challenges in the developing countries such as Nigeria (Davies, 2010). Waste if not properly disposed could lead to contamination of surface and groundwater in its immediate environment (Camacho et al., 2011).

Abstraction of groundwater from both soft and hard rock environment is mainly through the identification of aquifers in the subsurface. In a hard rock environment (that is, a crystalline bedrock setting), aquifers are located within a very thick weathered overburden and/or fractured bedrock (Sunmonu et al., 2012). To reduce the risks of uncertainties surrounding the location of aquifers in the subsurface, geophysical methods such as electromagnetic, electrical resistivity, magnetic, and gravity methods have been adopted in such quest (Raji, 2014; Adagunodo et al., 2018a). One of the most important environmental issues today is groundwater contamination (Adagunodo 2017), and between the wide diversity of contaminants affecting water resources, waste materials (of diverse contents) constitute the larger percent of these contaminants. Some of the waste materials are enriched in radon concentrations contributing to groundwater contamination by radon (Ahmed et al., 2019). The UNSCEAR Report in 2006 disclosed that when groundwater and surface water were assessed, 20% of groundwater samples were polluted with radon gas while 0.2% was recorded for surface water samples (UNSCEAR, 2006). Water from crystalline basement aquifers could contain radon due to the composition of radioactive materials in the basement rocks (Shu'aibu et al., 2021). The geological rocks of southwestern Nigeria are rich in ^{226}Ra , which is the direct parent of ^{222}Rn (Esan et al., 2020; Oladapo et al., 2022). This could be a medium for record of elevated radon concentrations in some locations within the southwest Nigeria.

Radon is a carcinogenic radioactive gas being formed by the decay of ^{238}U (Oni and Adagunodo, 2019). It is present from point to point in differs quantity within the crust (Abodunrin and Akinloye, 2020). It escapes to the soil through the fractured bedrocks, rock pores, and faults; and to the groundwater through the aquifer pores and soil pores; whereby it diffuses into the air from the surface of the Earth (Shu'aibu et al., 2021; Oladapo et al., 2022). Low radon concentrations are associated with wet or moist soils and compacted geological formations (that could have attained equilibrium based on its time of deposition) that are older than 1600 years, being the half-life of ^{238}U (Abodunrin and Akinloye, 2020). The radon being emanated from the subsurface is high in dry soils, unconsolidated deposits, shallow surface strata, and specific types of bedrocks (such as shales, limestones, permeable sandstones, granites, sedimentary ironstones, and phosphatic rocks that are rich in uranium), and in shallow surface strata (Tanner, 1964; Narayana et al., 2007; Ferreira et al., 2011; Saç et al., 2012; Ademola and Oyeleke, 2017).

The World Health Organization (WHO, 2009) and the International Commission on Radiological Protection (ICRP, 2009) had described inhalation of high concentrations of radon as the second leading causative agent for lung cancer, with smoking being the major cause (WHO, 2009; ICRP, 2009; Oni et al., 2019a; Yusuff et al., 2019; Oni et al., 2021; Oruncak and Ozkan, 2020; Usikalu et al., 2020; Modibo et al., 2021).

The carcinogenic havoc caused by radon to lungs varied from 3 to 17% of the total life threatening diseases that had been recorded (Sharma et al., 2016). In fact, 57% of the attack to lungs is as a result of radon inhalation and its degradation products (Oruncak and Ozkan, 2020). A great number of deaths had been recorded in the United States of America due to overexposure to radon (Usikalu et al., 2020). The numbers of lung cancer's deaths being associated with radon exposure in Norway has increased by 12% (Finne et al., 2019). An increase of 5.9%, 7.0%, 6.2% and 6.1% deaths had been recorded in Turkey, Poland, Hungary, and Armenia, respectively (Gaskin et al., 2018). In Norway, an increase of 12% lung cancer's death had been recorded (Grundy et al., 2017), and up to 16% increase in death rate associated with radon exposure had been recorded in Canada (Health Canada, 2018) and in France (Airouche et al., 2018). Studies on radon concentrations from point to point and its health effects are not only advantageous in the environmental and health sector, they are also useful in mining, geosciences, ore exploration, identification of major faults, forecasting of earthquake occurrences, and subsurface integrity check prior to building constructions (Igarashi et al., 1995; Lawrence et al., 2009; Hwa and Kim, 2015; Chambers et al., 2018; Saad et al., 2020; Modibo et al., 2021; Sakr et al., 2022; Sukanya et al., 2022).

Awareness of the presence of radon and its potential health effects is very low in Nigeria. High radon concentrations in drinking water have been linked to stomach cancer (Ademola and Oyeleke, 2017). Though there are numbers of publications on the risk assessments of radon in the Nigerian groundwater system (Oni and Adagunodo, 2019; Oni et al., 2019b; Bello et al., 2020; Ajibola et al., 2021; Shu'aibu et al., 2021; Oni et al., 2021), little or no report was documented within the vicinity of the study area. This paper shall serve as a baseline study that has considered the effect of dumpsite on the degree of radon concentrations in the groundwater around a mega dumpsite. It would also seek to achieve some of the Sustainable Development Goal's (SDG) agenda such as SDG 3, 11 and 12. These three SDG were constituted in order to attain the following feats by the year 2030: assurance of healthy lives and promotion of well being for all ages; ensuring that cities and human settlements are safe and sustainable; and by establishing a sustainable consumption pattern (SDG, 2019). The use of un-treated groundwater capable of having high radon concentrations for drinking and other domestic purposes is usually being practised in the south-western region of Nigeria. Thus an exposure to radon from un-treated water could result to accumulation of high absorbed doses in some gastrointestinal tract organs (such as stomach, rectum, anus, small and large intestines) and some tissues (such as the lining of the gastrointestinal tract and lung tissues) (Hopke et al., 2000; Oni et al., 2019b; Suresh et al., 2020). Recent study by Zhang et al. (2022) posited that there are plausible linkages between radon exposure and development of dementia in humans. This study was conceived with the aim to assess the radiological health effects of water consumed and used for domestic purposes as well as to investigate the radon source(s) or pathway(s) in shallow aquifers within granitic rocks from two settlements in the crystalline basement complex of Nigeria.

1.1. Description of study area and its geological settings

Ibadan, the acclaimed largest city in the West Africa, is bounded by the Republic of Benin in the west and other Nigerian state boundaries in its other axes (Oladejo et al., 2019). It is the second most congested city to Lagos in Nigeria with the total geographical area and population of about 6800 km² and 2.84 million people (Ademola and Oyeleke, 2017). It is one of the mega cities being situated within the humid and sub-humid tropical climate in southwestern Nigeria. The annual rainfall

and the maximum temperature in Ibadan are approximately 1230 mm and 32 °C, respectively (Aladejana et al., 2018).

The geology of Ibadan is that of the PreCambrian basement complex (Fig. 1a) which is an integral of the reformed basement rocks of West Africa (Adagunodo et al. 2018a, 2018b, 2019a). The predominant rocks of the basement complex are mainly metamorphic and crystalline rocks (Adagunodo et al., 2013; 2013). In Ibadan, some intrusive rocks such as granites and porphyries are found within the metamorphic rocks (Ganiyu et al., 2018). As shown in Fig. 1b, the rocks within Ibadan and its environs are: amphibolites, undifferentiated gneiss complex, migmatite and banded gneiss, granite gneiss, pegmatite and quartz vein as

well as quartzite quartz schist (Okunlola et al., 2009). Migmatite and banded gneiss are the major rocks in Ibadan. These major rocks are originated from a highly altered metamorphic rock that is banded or mixed with granitic rocks.

The study area is situated at the southeastern region of Ibadan (Fig. 1b). About 7 m away from the dumpsite, there is a river flowing in W – E direction. The plumes from the dump could have infiltrated into the river through the fault lines around study site (Fig. 1b). The study area is situated in a very low land with a valley-like topography being experienced towards its northwestern side. Locally, Amuloko and its environs are generally underlain with a very thin overburden (Aladejana

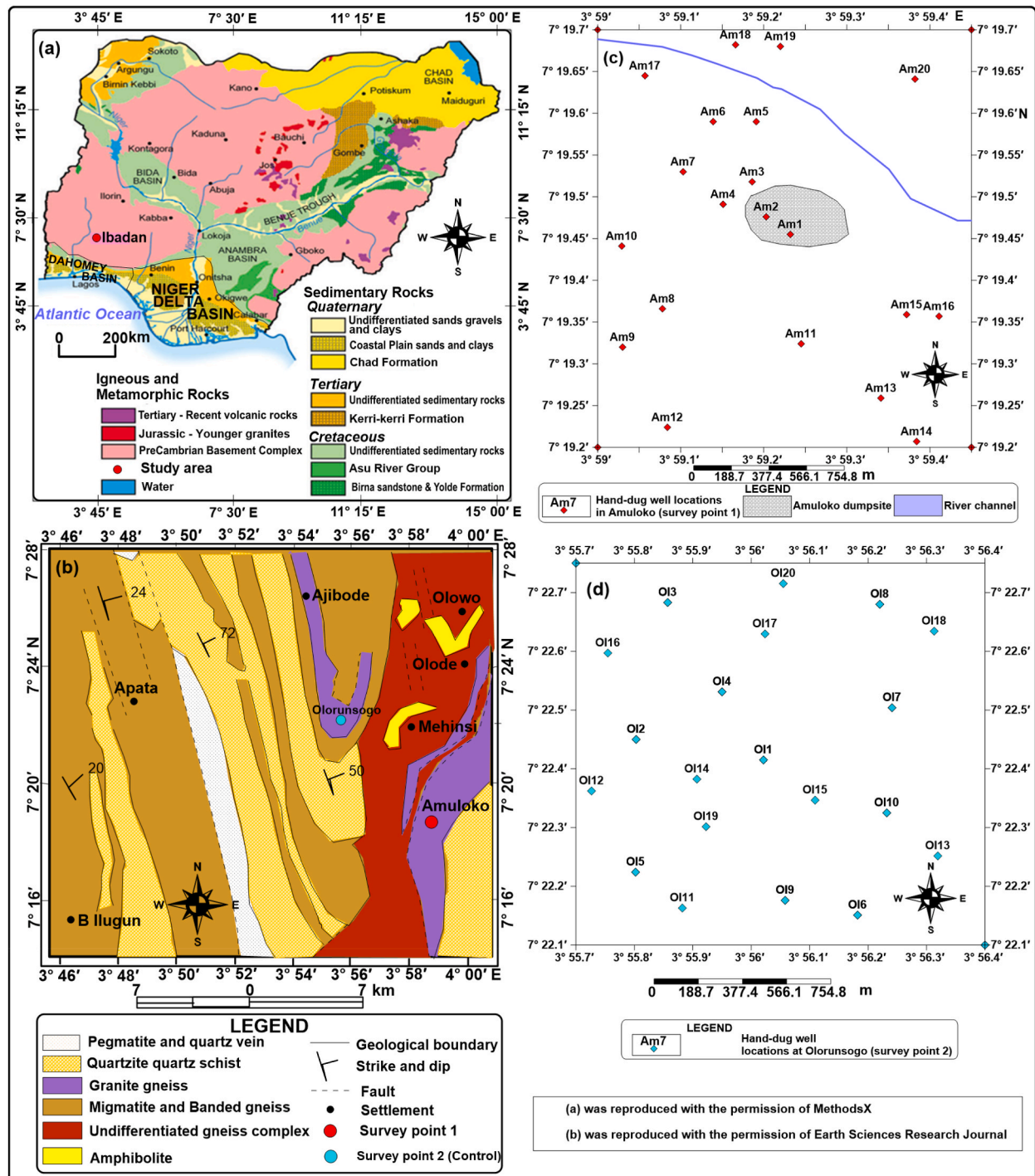


Fig. 1. Various maps showing the area of study: (a) Geological map of Nigeria (adapted from Adagunodo et al., 2019a), (b) Geological map of Ibadan (reproduced from Okunlola et al., 2009), (c) Base map of survey point 1 in Amuloko area, (d) Base map of survey point 2 in Olorunsogo.

et al., 2018). The granite gneiss constitutes the geology of the study area. Gneiss is a metamorphic rock that was formed under enormous heat and pressure. It is formed from granites, volcanics or schists. It is made up of coarse-grained minerals such as feldspar and quartz. The composition of granitic gneiss resembles that of granite.

The hydrogeologic conditions that control the storativity and transmissivity of the study area are the same as that of basement rocks. In basement complex rocks, aquifers are concealed within the weathered and/or fractured bedrocks (Sunmonu et al., 2012). At the unaltered state of the basement complex rocks, they are characterized by low porosity and permeability. As soon as they become weathered and fractured, secondary porosity and permeability are developed which now controls the flow and storativity of groundwater within the aquifers of basement rocks (Lapworth et al., 2017; Adagunodo et al., 2018a). The depth to water table and the elevation of the study area varied from 1.0 to 6.0 m and 150–167 m, respectively.

2. Materials and methods

A total of forty (40) water samples were obtained from Amuloko and Olorunsogo in Ibadan. Twenty (20) water samples were taken from hand-dug wells starting from the closest residential building to Amuloko dumpsite to other residential areas within the study site. In order to assess the sources of the radon concentrations into the groundwater system in the study area, twenty (20) water samples were obtained in Olorunsogo area (about few kilometers away from Amuloko) in Ibadan. The water samples were collected at the early hours of the day (before the commencement of human activities) for an in-situ analysis of each hand-dug well. The early-hour analysis was done to ensure that some properties of the water were not affected by human activities. A clean 1.5 L plastic bottle was used for each sample collection. All the bottles used were rinsed with distilled water a day to the sample's collection. It was ensured while dipping the bottles in a fetcher that the water bubbles were prevented from being entrapped into the bottle prior to its capping to avoid escape of dissolved radon in the water (Oni et al., 2019b). For accuracy, three (3) water samples were taken at each location (culminating to a total of 120 samples in all locations), where the mean of the result obtained was used as the representative value for each location. The collected samples were analyzed before the sun rises on daily basis. This is to ensure that the quality of the obtained results is unaltered, as temperature increase could affect the level of radon concentrations in water (Ajibola et al., 2021; Orosun et al., 2021).

A well-calibrated active electronic detector (RAD7) was used for in-situ measurements of radon concentrations in each water sample. The set-up of the RAD7 used in this study is shown in Fig. 2 (Durrige, 2013). RAD7 is a semiconductor detector that uses the principle of Alpha spectroscopy method for its measurements. It measures radon daughters that accumulate on the detector surface with a strong electric field. RAD7 is an accurate sniffer that can be used for both short-term and long-term measurements. It is capable of dissolving the energy of various radon isotopes such as radon (Radon-222) and thoron (Radon-220). In Big Bottle System, a bottle varying from 1.5 to 2.5 L could be fixed to the detector (Durrige, 2013, 2018a). In this study, a 1.5 L bottle, as utilized by Orosun et al. (2021), was adopted. The Big Bottle System uses a closed loop aeration process. This process resembles that of RADH₂O system. In a closed loop aeration process, at all time, there are constant volumes of water and air with an independent flow rate. As the air re-flows through the water, radon concentrations are extracted from the water until a state of equilibrium is reached. It takes 10 min aeration to attain equilibrium unlike in RADH₂O system that aeration only takes 5 min (Durrige, 2018b). Also, the time for aeration is very short in comparison to 3.8 days half-life of radon. This quality gives RAD7 an edge over other detectors for measuring radon in water.

Prior to the measurement of radon concentrations in the water samples, the entrapped radon and dry air were purged from the active electronic detector (RAD7) through the help of the drying unit.

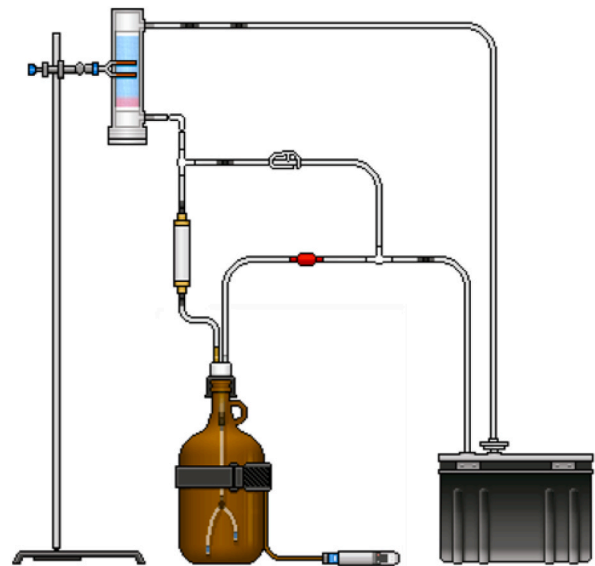


Fig. 2. An experimental set-up for measuring radon in water using RAD7 (Adapted from Durrige, 2018b).

Afterwards, each 1.5 L plastic bottle filled with the collected sample was fixed to the drying unit and the detector. The device was allowed to function in a Sniff mode in order to determine the concentrations of radon inside the air loop. After the radon in the air loop has been determined, the conversion factor from the Big Bottle System (substituting 1.5 L plastic bottle for 2.5 L) and the water's temperature during aeration were used to determine the concentration of radon in each water sample (Durrige, 2018a). The Durrige's CAPTURE package was used for this process, because by using the Big Bottle System, the radon in the air loop is easily determined and automatically estimate the concentrations of radon in the water (Durrige, 2018b). To assess the relationship between some physical parameters (such as temperature and pH) and radon concentrations in the study locations, thoron concentrations were measured by RAD7 detector. Apart from the half-life of thoron (55.6 s) that is shorter than that of radon (3.8 days), both elements are identical for all experimental activities (Lane-Smith and Schubert, 2020). This permits thoron to be measured by RAD7 using alpha spectrometry method as well. The groundwater pH and its corresponding temperature were measured on-site by using the Hanna meter. RAD7 has a measurement accuracy of $\pm 5\%$, a nominal sensitivity of $0.00925 \text{ Bq l}^{-1}$ and an intrinsic background of $0.000185 \text{ Bq l}^{-1}$ (DURRIDGE, 2018a).

The radiation doses due to ingestion and inhalation were estimated for all the water samples. This is imperative because either of the two could cause serious health issues besides the lung cancer as soon as it is absorbed into the bloodstreams (Hopke et al., 2000). The annual effective dose for radon ingested is calculated using equation (1) as given by UNSCEAR (2000) as well as Ademola and Oyeleke (2017).

$$\text{AEDR}_{\text{ing}} (\mu\text{Sv y}^{-1}) = (\text{CRn})_{\text{w}} \times (\text{C})_{\text{w}} \times (\text{EDC}) \quad (1)$$

where AEDR_{ing} is the annual effective dose of radon ingested, $(\text{CRn})_{\text{w}}$ is the radon concentrations in drinking water (kBq m^{-3}), $(\text{C})_{\text{w}}$ is the "annual" water intake (given as 0.5, 1.5 and 2.0 L of water per day by infants, children and adults, respectively) (WHO, 2004, 2011; Duggal et al., 2013; Bem et al., 2014). The choice of water intake per person can vary based on daily activities or season (Howard and Bartram, 2003). The values adopted in this study are as a result of the physical activities, climate and culture of people residing in Ibadan, Nigeria. The EDC is the effective dose conversion coefficients (given as 7×10^{-8} , 2×10^{-8} and $1 \times 10^{-8} \text{ Sv Bq}^{-1}$ for infants, children and adults, respectively) (UNSCEAR 2000; Ezzulddin and Mansour, 2017)

The annual effective dose of radon inhaled is calculated using equation (2) as given by UNSCEAR (2000) as well as Ezzulddin and Mansour (2017).

$$AEDR_{inh} (\mu Sv y^{-1}) = (CRn)_w \times (Rn)_w \times (Eq) \times (IOT) \times (DCF) \quad (2)$$

where $AEDR_{inh}$ is the annual effective dose of radon inhaled, $(Rn)_w$ is the radon in air-to-water (given as 10^{-4}), (Eq) is the equilibrium factor between radon and its decay products (given as 0.4), (IOT) is the mean indoor occupancy time per person (given as 7000 hy^{-1}) and (DCF) is the dose conversion factor for being exposed to radon (given as $9 \text{ nSv h}^{-1} (\text{Bq m}^{-3})^{-1}$) (Ademola and Oyeleke, 2017; Orosun et al., 2021).

In order to have a clue about the overall doses being received through radon ingested and radon inhaled annually, equation (3) is used to estimate the annual effective dose of total radon received $(AEDR)_{total}$.

$$(AEDR)_{total} (\mu Sv y^{-1}) = (AEDR)_{ing} + (AEDR)_{inh} \quad (3)$$

Kriging was used for the production of geospatial maps in this study. Kriging is a geostatistical gridding technique in numerical analysis that has proven useful in other fields (Omosehinmi and Arogunjo, 2016). It produces the most appealing linear unbiased prediction (and visual maps) at unsampled locations (Surfer Version, 2021). It could be used to

measure the uncertainty in the estimated surface and to also measure the spatial correlation between two points (Wu and Hung, 2016). The application of this geostatistical approach has been shown by many authors (Sunmonu et al., 2012; Adagunodo et al., 2018a).

The basic descriptive statistics such as the mean, standard deviation (SD), coefficient of variation (CV), skewness (skew.), kurtosis (kurt.), minimum (min.), maximum (max.), t -test and the analysis of variance (ANOVA) were performed on the raw and processed data in order to determine the intra-variation among the data and the inter-variation that exist between the data that were acquired on the two granitic terrains (that is, Amuloko and Olorunsogo, Ibadan). Descriptive analysis had been one of the useful tools to describe in summary the variations that exist between set of obtained or acquired data (Ademola and Oyeleke, 2017; Adagunodo et al., 2019b; Orosun et al., 2021; Ghias et al., 2021).

3. Results and discussion

The geospatial distributions of radon concentrations in water $(CRn)_w$ and the annual effective dose from radon concentrations (AEDR) by infants, children and adults through ingestion and inhalation within

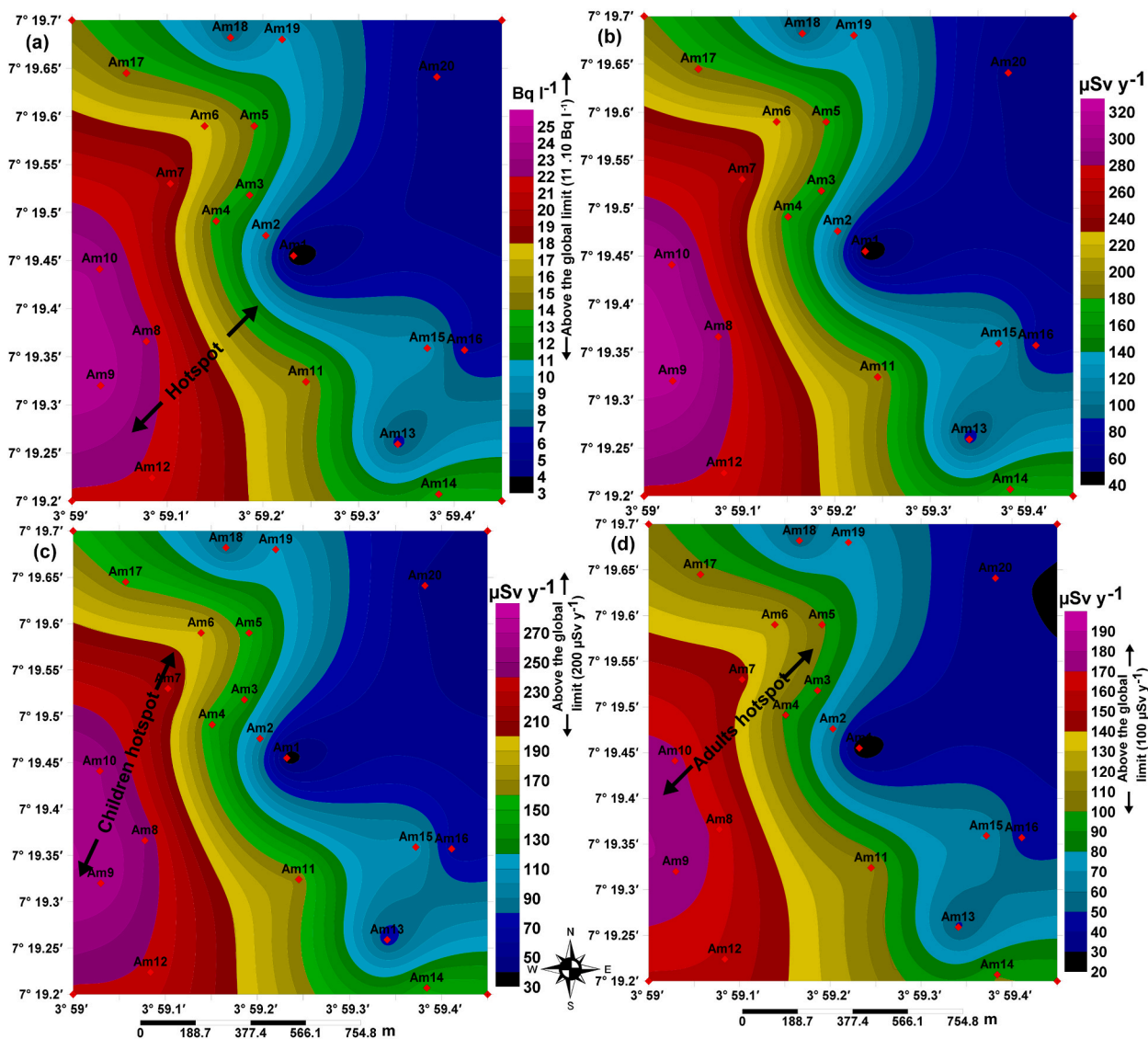


Fig. 3a. AEDR maps around Amuloko dumpsite (a) Radon in Amuloko water (b) Radon ingested by infants in Amuloko water (c) Radon ingested by children in Amuloko water (d) Radon ingested by adults in Amuloko water.

Amuloko and Olorunsogo and its environs are shown in Fig. 3a–h and Fig. 4-h, respectively. The radon concentrations in Amuloko groundwater trend in the North East (NE) to South West (SW) orientation. Very low radon concentrations are observed at the Amuloko dumpsite and around the river channel. This implies that the dumpsite is acting as an artificial lining that suppresses radon emission around the dumpsite. Also, radon concentrations in surface water are comparably lower than that of groundwater (Oni et al., 2019a; Ajibola et al., 2021). Majorly, the north-western, western, south-western and southern parts of the study area in Amuloko are notable hotspots. The radon concentrations in groundwater sources from the hotspots in Amuloko (Fig. 3a–h) are beyond the global limits of 11.10 Bq l^{-1} for radon concentrations in water $(\text{CRn})_w$, 100.00 and $200.00 \mu\text{Sv y}^{-1}$ for the AEDR ingested in water by adults and children as given by the UNSCEAR (2000). The concentrations of radon in Amuloko groundwater increased towards the fault line between the undifferentiated gneiss complex and granite gneiss in the study area (Fig. 1b). The results in the groundwater sources from Amuloko corroborate with the claim that radon emits more along fault lines (Choubey et al., 2000; Al-Tamimi and Abumurad, 2001; Prasad et al., 2009; Chen et al., 2018; Sukanya et al., 2022).

The radon concentrations in the groundwater sources in Olorunsogo area increase towards the north-eastern direction (Fig. 4a–h). Low concentrations of radon from different groundwater sources are observed towards the south-western part of the survey point 2 (Olorunsogo). There are hotspots at the northern, north-eastern, eastern and part of the south-eastern zones. The obtained results from the hotspot zones are higher than the average global limits of 11.10 Bq l^{-1} for radon concentrations in water $(\text{CRn})_w$, 100.00 and $200.00 \mu\text{Sv y}^{-1}$ for the annual effective doses of radon (AEDR) ingested in water by adults and children as given by the UNSCEAR (2000). Like in Amuloko results, the radon concentrations in groundwater sources in Olorunsogo also increased towards the fault line within the basement rocks (Fig. 1b). The level of radon concentrations along these two faults further confirmed that granitic rocks are associated with high radon contents (Choubey et al., 2000; Omeje et al., 2019; Oni et al., 2019a).

The estimated basic descriptive statistics for the annual effective dose of radon received (AEDR) in water in Amuloko area (survey point 1) and in Olorunsogo (survey point 2) are presented in Tables 1 and 2. At survey point 1 (Amuloko), the minimum (min.) and maximum (max.) values for the $(\text{CRn})_w$ varied from 3.00 to 24.50 Bq l^{-1} with mean and standard deviation (SD) of $13.45 \pm 6.58 \text{ Bq l}^{-1}$. The min. And max. values for the $(\text{AEDR})_{\text{ing}}$ in water by infants, children and adults varied

The radon concentrations in the groundwater sources in Olorunsogo

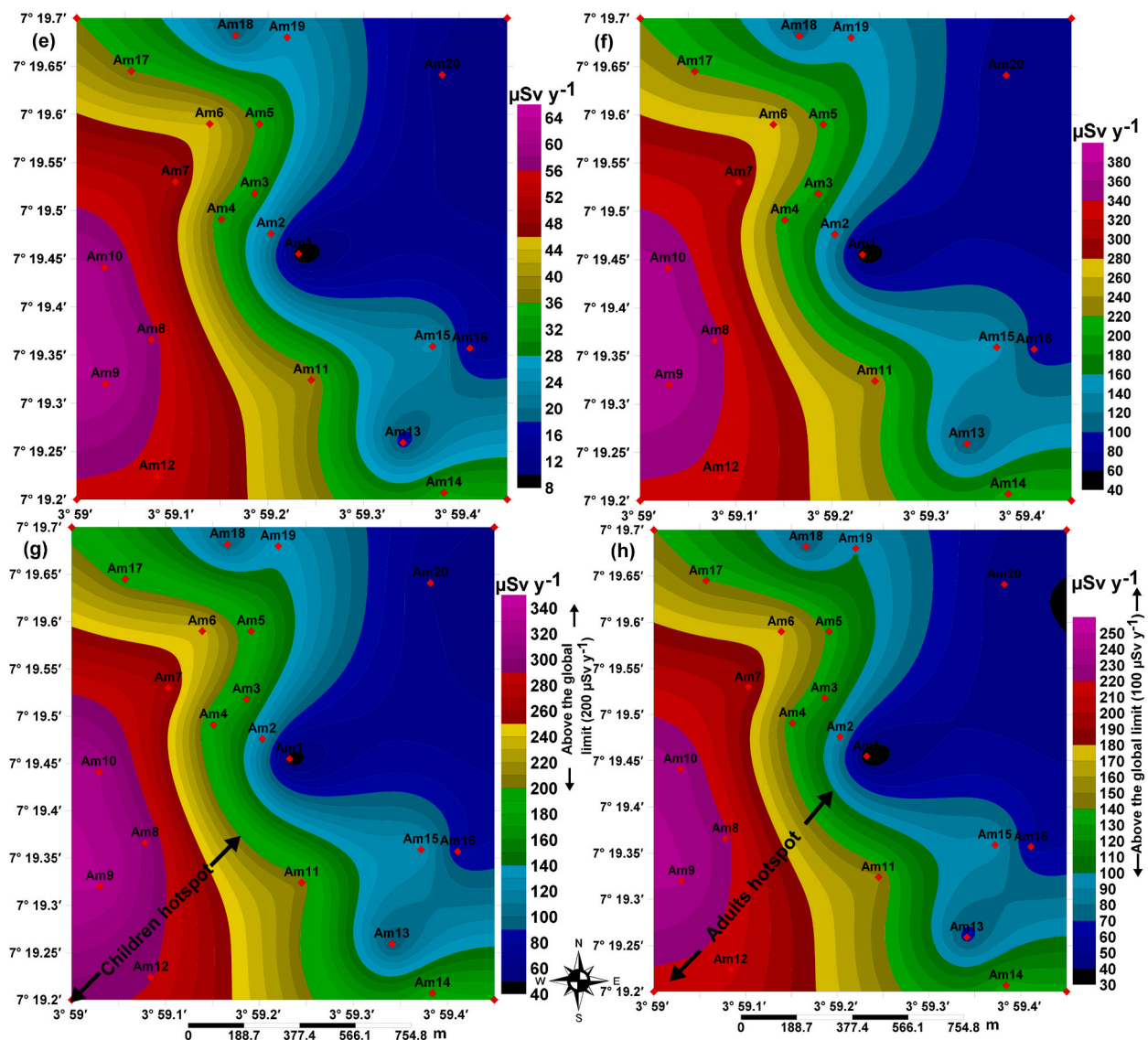


Fig. 3b. AEDR maps around Amuloko dumpsite (e) Radon inhaled in Amuloko water (f) Total radon received by infants in Amuloko water (g) Total radon received by children in Amuloko water (h) Total radon received by adults in Amuloko water.

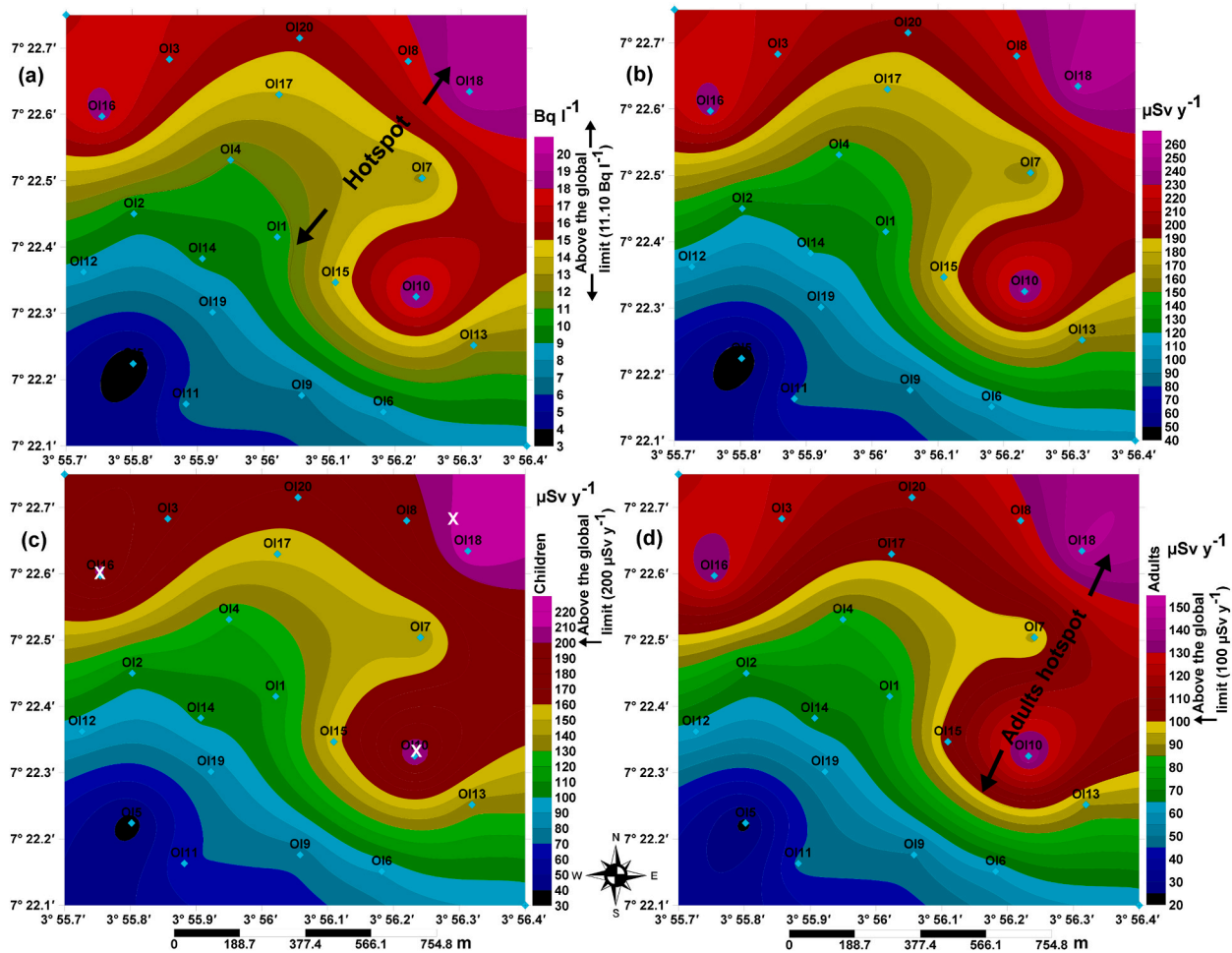


Fig. 4a. AEDR maps far off Amuloko (Olorunsogo area) (a) Radon in Olorunsogo water (b) Radon ingested by infants in Olorunsogo water (c) Radon ingested by children in Olorunsogo water (d) Radon ingested by adults in Olorunsogo water.

from 38.36 to 313.01 $\mu\text{Sv y}^{-1}$, 32.88–268.30 $\mu\text{Sv y}^{-1}$ and 21.92–178.86 $\mu\text{Sv y}^{-1}$, respectively. The mean and SD of the $(\text{AEDR})_{\text{ing}}$ in water by these three age groups are $171.80 \pm 84.07 \mu\text{Sv y}^{-1}$, $147.26 \pm 72.06 \mu\text{Sv y}^{-1}$ and $98.17 \pm 48.04 \mu\text{Sv y}^{-1}$, respectively. The min. And max. values of the $(\text{AEDR})_{\text{inh}}$ in water varied from 7.57 to 61.75 $\mu\text{Sv y}^{-1}$ with mean and SD of $33.89 \pm 16.58 \mu\text{Sv y}^{-1}$. The min. And max. values of the $(\text{AEDR})_{\text{total}}$ received in water through inhalation and ingestion by infants, children and adults varied from 45.93 to 374.76 $\mu\text{Sv y}^{-1}$, 40.45–330.04 $\mu\text{Sv y}^{-1}$ and 29.49–240.61 $\mu\text{Sv y}^{-1}$, respectively. The mean and SD of the $(\text{AEDR})_{\text{total}}$ received in water by these three age groups are $205.69 \pm 100.65 \mu\text{Sv y}^{-1}$, $181.15 \pm 88.64 \mu\text{Sv y}^{-1}$ and $132.06 \pm 64.62 \mu\text{Sv y}^{-1}$, respectively. The high observed SD in this study could be attributed to the heterogeneity of the near-surface layers of the crust (Ali et al., 2010; Khan 2011; Orosun et al., 2021; Oladapo et al., 2022).

At survey point 2 (Olorunsogo), the lowest and the highest values for the $(\text{CRn})_{\text{w}}$ varied from 3.18 to 20.00 Bq l^{-1} with an average and standard deviation (SD) of $12.06 \pm 4.74 \text{Bq l}^{-1}$. The lowest and the highest values of the $(\text{AEDR})_{\text{ing}}$ in water by infants, children and adults varied from 40.56 to 255.53 $\mu\text{Sv y}^{-1}$, 34.77–219.02 $\mu\text{Sv y}^{-1}$ and 23.18–146.01 $\mu\text{Sv y}^{-1}$ in sequence. The averages and standard deviations of the $(\text{AEDR})_{\text{ing}}$ in water by these three age groups are $154.12 \pm 60.58 \mu\text{Sv y}^{-1}$, $132.10 \pm 51.93 \mu\text{Sv y}^{-1}$ and $88.07 \pm 34.62 \mu\text{Sv y}^{-1}$, respectively. The lowest and the highest values of the $(\text{AEDR})_{\text{inh}}$ in water varied from 8.00 to 50.41 $\mu\text{Sv y}^{-1}$ with an average and SD of $30.40 \pm 11.95 \mu\text{Sv y}^{-1}$. The lowest and the highest values of the $(\text{AEDR})_{\text{total}}$ received in water through inhalation and ingestion by infants, children

and adults varied from 48.56 to 305.93 $\mu\text{Sv y}^{-1}$, 42.77 and 269.43 $\mu\text{Sv y}^{-1}$ and 31.18–196.42 $\mu\text{Sv y}^{-1}$ in sequence. The averages and standard deviations of the AEDR received in water by these three age groups are $184.52 \pm 72.53 \mu\text{Sv y}^{-1}$, $162.51 \pm 63.88 \mu\text{Sv y}^{-1}$ and $118.47 \pm 46.57 \mu\text{Sv y}^{-1}$, respectively.

At the two survey points (Amuloko and Olorunsogo), the estimated mean values for the $(\text{CRn})_{\text{w}}$ are higher than the global limit (GL) of 11.10 Bq l^{-1} by factors of 1.21 and 1.09, respectively. This shows that the groundwater at the two granitic locations is enriched with radon. Consumption of elevated concentrations of radon in water for all age groups had been linked to serious health challenges such as lung cancer and stomach cancer (UNSCEAR, 2000; Al-Tamimi and Abumurad, 2001; WHO, 2018; Oni and Adagunodo, 2019; Ajibola et al., 2021; Oni et al., 2021). Furthermore, the mean values for $(\text{AEDR})_{\text{total}}$ by adults at the two survey points are higher than the GL of 100 $\mu\text{Sv y}^{-1}$ by factors of 1.32 and 1.19, respectively. The order of the mean AEDR received in water by all age groups from Tables 1 and 2 revealed that infants > children > adults. The overall outcome of this order constitute deleterious health hazard to infants in both locations because some of the critical organs in infants are radio-sensitive, since some of these organs have not been fully developed. Generally, the mean AEDR that is higher than 100 $\mu\text{Sv y}^{-1}$ in water is considered as being unsafe for consumption by all age groups (infants, children and adults) (USEPA, 1999; WHO 2004; Nasir and Shah, 2012; Ademola and Oyeleke, 2017). The trend of results in all age groups in this study is in agreement with the studies conducted on Precambrian basement rocks by Ajibola et al. (2021) and Orosun et al. (2021).

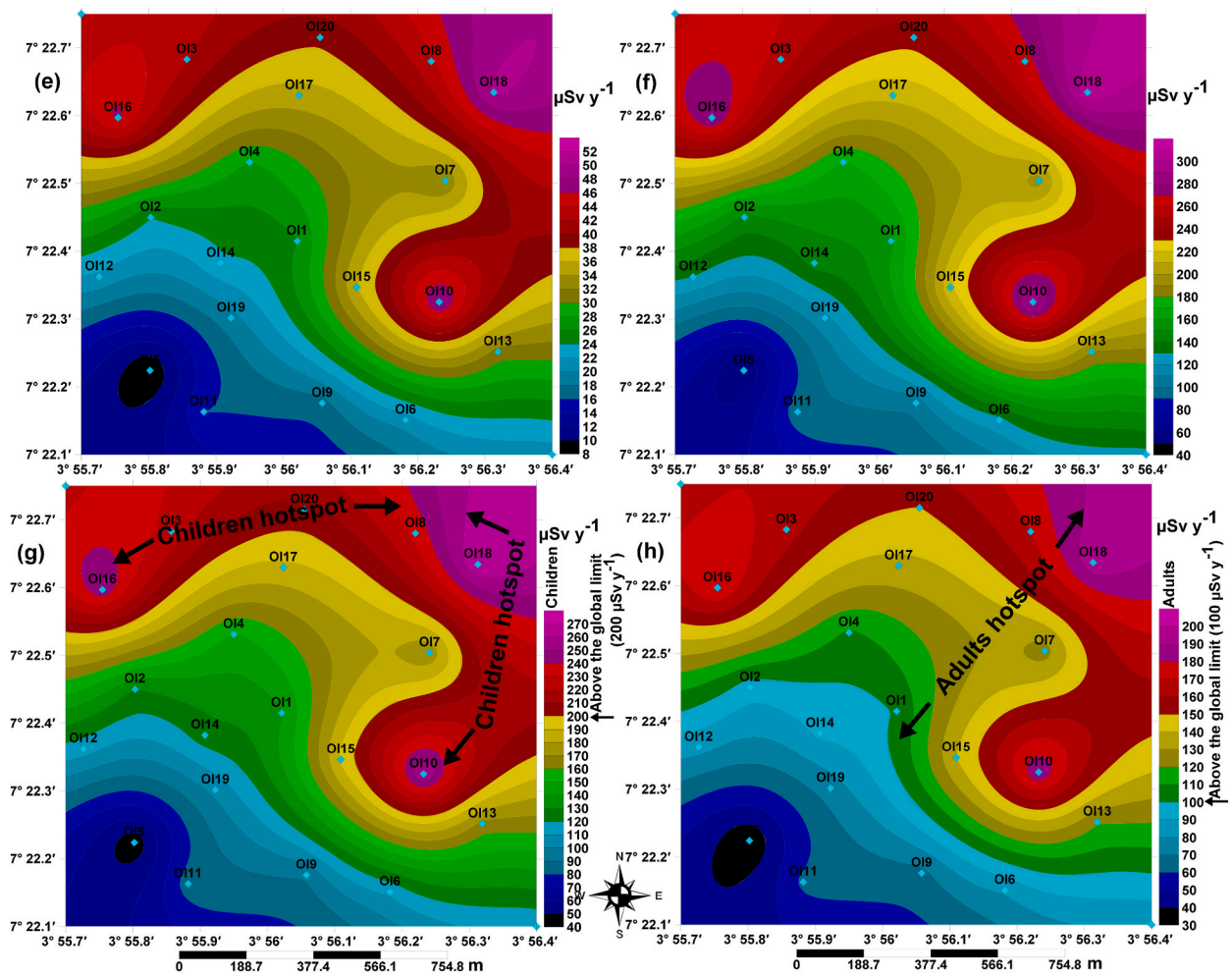


Fig. 4b. AEDR maps far off Amuloko (Olorunsogo area) (e) Radon inhaled in Olorunsogo water (f) Total radon received by infants in Olorunsogo water (g) Total radon received by children in Olorunsogo water (h) Total radon received by adults in Olorunsogo water.

Table 1
Basic descriptive analysis for AEDR in water around Amuloko dumpsite.

N = 20	Min.	Max.	Mean ± SD	Median	CV	Skew.	Kurt.	GL
A	3.00	24.50	13.45 ± 6.58	13.43	0.49	0.22	-0.97	11.10 *
B	38.36	313.01	171.80 ± 84.07	171.57				NA
C	32.88	268.30	147.26 ± 72.06	147.06				200.00 *
D	21.92	178.86	98.17 ± 48.04	98.04	0.49	0.22	-0.97	100.00 *
E	7.57	61.75	33.89 ± 16.58	33.84				NA
F	45.93	374.76	205.69 ± 100.65	205.41				NA
G	40.45	330.04	181.15 ± 88.64	180.90				200.00 *
H	29.49	240.61	132.06 ± 64.62	131.88				100.00 *
I	25.30	31.50	28.14 ± 1.78	27.40	0.07	0.63	-0.56	24.5-39.7 **
J	7.00	7.40	7.16 ± 0.12	7.15	0.02	0.25	-0.95	6.8-8.5 **
K	0.44	1.56	0.84 ± 0.37	0.72	0.44	0.99	-0.17	NA

Note: Min. = Minimum, Max. = Maximum, SD = Standard deviation, CV = Coefficient of variation, Skew = Skewness, Kurt = Kurtosis, GL = Global limit, A = (CRn)w (Bq l-1), B = (AEDR)ing (μSvy-1) by infants, C = (AEDR)ing (μSvy-1) by children, D = (AEDR)ing (μSvy-1) by adults, E = (AEDR)inh (μSvy-1), F = (AEDR)total (μSvy-1) by infants, G = (AEDR)total (μSvy-1) by children, H = (AEDR)total (μSvy-1) by adults, I = Temperature (°C), J = pH, K = Thoron (Bq l-1), * = UNSCEAR (2000), ** = WHO (2011), NA = Not available.

The coefficient of variation (CV) is a statistical measure of the dispersion of the available data around the mean. It is the ratio of the SD to the mean. The coefficient of variation (CV) is a useful tool for comparing the variation levels between intra-data points and inter-data points. A $0 \leq CV \leq 0.1$ implies a low level of variation, $0.11 \leq CV \leq 0.30$ implies a medium level of variation and $0.31 \leq CV \leq 1$ implies a high level of variation (Wang et al., 2017). A low level of variation indicates intra-variation while a high level of variation indicates inter-variation

(Machin et al., 2007). The intra-data variations (variations within the data per location) that produced the CV of 0.49 in Amuloko area and 0.39 in Olorunsogo area indicates that radon is not part of the groundwater's constituent but a foreign body that find its way into the aquifer. Meanwhile, a difference of 0.05 is observed in the CV between the two locations (inter-data variation). This further confirms that the radon concentrations emanating from the two locations are from the same source. This suggests that the anthropogenic activities around the survey

Table 2
Basic descriptive analysis for AEDR in water far off Amuloko (Olorunsogo area).

N = 20	Min.	Max.	Mean \pm SD	Median	CV	Skew.	Kurt.	GL
A	3.18	20.00	12.06 \pm 4.74	11.68	0.39	0.09	-0.88	11.10 *
B	40.56	255.53	154.12 \pm 60.58	149.15				NA
C	34.77	219.02	132.10 \pm 51.93	127.85				200.00 *
D	23.18	146.01	88.07 \pm 34.62	85.23	0.39	0.09	-0.88	100.00 *
E	8.00	50.41	30.40 \pm 11.95	29.42				NA
F	48.56	305.93	184.52 \pm 72.53	178.58				NA
G	42.77	269.43	162.51 \pm 63.88	157.27				200.00 *
H	31.18	196.42	118.47 \pm 46.57	114.65				100.00 *
I	33.20	36.50	34.96 \pm 0.95	34.70	0.03	0.08	-0.73	24.5–39.7 **
J	6.50	7.10	6.79 \pm 0.19	6.80	0.03	0.16	-1.21	6.8–8.5 **
K	0.31	1.21	0.59 \pm 0.20	0.55	0.34	1.58	3.77	NA

Note: Same interpretation for Table 1 is applicable to Table 2.

point 1 do not contribute to the level of radon gas in Amuloko groundwater sources.

Skewness (skew.) and kurtosis (kurt.) are integral of data characterization (Adagunodo et al. 2019b). The skewness determines the equivalence or non-equivalence of data. The kurtosis compares the peakedness or flatness (tailedness) of a set of distribution to a normal distribution. The skewness in Amuloko and in Olorunsogo areas are 0.22 and 0.09, indicating asymmetric right skewed probability distributions at the two locations. A right skewed data implies that its right tail is longer when compared to its left counterparts (Groeneveld and Meeden, 1984). At the two locations, the distributions are normally distributed about the mean since ± 1 indicates the range of comfortability in normality test (Normality Testing, 2019). The kurt. At survey points 1 and 2 are -0.97 and -0.88, indicating flattened (light-tailed) distributions. As reported by Ghias et al. (2021), a light-tailed distribution goes along with a low kurt., which corresponds to the results obtained in this study.

The pH of groundwater from Amuloko varied from 7.0 to 7.4 with a mean of 7.2 (Table 1). Meanwhile, the pH from Olorunsogo groundwater varied from 6.5 to 7.1 with a mean of 6.8 (Table 2). The results from the two locations suggest that the pH of groundwater in Amuloko is of weakly alkaline while that of Olorunsogo varied from weakly acidic to weakly alkaline. The influence of waste site could have resulted to a weak alkalinity nature of Amuloko groundwater (Olafisoye et al., 2012). Results from the two locations are within the acceptable limits by WHO which varied from 6.8 to 8.5 (WHO, 2011). The pH values of groundwater from this present study are in agreement with the pH of groundwater obtained from a granitic environment in Ogbomoso, south-west Nigeria (Adabanija et al., 2020). One of the physical parameters that determine the suitability of water for human consumptions and other applications is water temperature. The WHO recommends that the temperature of water for human use should vary from 24.5 to 39.7 °C (WHO, 2011). The water temperature in Amuloko ranged between 25.3 and 31.5 °C with a mean of 28.1 °C (Table 1), while that of Olorunsogo varied from 33.2 to 36.5 °C with a mean of 35.0 °C (Table 2). The results indicated that the groundwater sources at the two settlements are suitable for human usage and consumption, which correspond to the water temperature (25.2–38.8 °C) obtained from near a major fault in Zarand, Iran by Rahimi et al. (2022).

Thoron (^{220}Rn) is a gas and a radioactive isotope of radon (^{222}Rn), which is being produced from byproducts of thorium. It decays by emission of an alpha particle and has a half-life of ≈ 56 s. It is also capable of destroying the DNA (deoxyribonucleic acid) which could lead to lung cancer and other respiratory challenges if inhaled into the lungs (Wanjala et al., 2021). The descriptive results of thoron concentrations at both settlements are presented in Tables 1 and 2. In Amuloko, the thoron concentrations varied between 0.44 and 1.56 Bq l^{-1} with a mean of 0.84 Bq l^{-1} , while the ^{220}Rn concentrations in Olorunsogo ranged from 0.31 to 1.21 Bq l^{-1} with a mean of 0.59 Bq l^{-1} . The range of thoron concentrations obtained in the current study is higher than the values

(0–0.07 Bq l^{-1}) obtained in groundwater samples from Kufa city in Iraq (Ali et al., 2012). Currently, there is no threshold limit for thoron concentration in potable water. It is advisable to ensure that its concentrations in water for consumption and other uses is as low as possible to avoid any health risk that could accompany an overdose of thoron through ingestion or inhalation in future (Ali et al. 2012; Lane-Smith and Schubert, 2020). One of the applications of thoron measurements in groundwater system is to determine the groundwater discharge pattern (Chanyotha et al., 2010; Lane-Smith and Schubert, 2020). The presence of thoron in all the groundwater samples in Amuloko and in Olorunsogo areas could have been attributed to network of the faults in the study area, because in crystalline basement complex, viable aquifers could only be developed through weathering or fracturing of the parent rocks (Sunmonu et al., 2012; Adagunodo et al., 2018a).

The relationships between radon, temperature, pH and thoron at the two locations were established using the Pearson's correlation. The correlation results are presented in Table 3. Classifications of the results are as follows: a positive strong correlation exists when $R \geq 0.8$; a positive significant correlation exists when $0.5 \leq R < 0.8$; a positive weak correlation exists when $0.3 \leq R < 0.5$; and an insignificant positive correlation exists when $R < 0.3$ (Orosun et al., 2019, 2021). When the conditions above are in the negative form, it shows a negative correlation among the group (Adagunodo et al., 2018c). A negative weak correlation of -0.4266 and -0.3190 exists between radon and temperature in Amuloko and in Olorunsogo areas, respectively. This confirmed that an increase in temperature would reduce the concentrations of radon in water (Ajibola et al., 2021). Also, a strong positive correlation of 0.8949 in Amuloko and a significant positive correlation of 0.5914 in Olorunsogo between radon and thoron concentrations ascertained that both are byproducts of rocks and lithostratigraphic units being enriched with radioactive elements (uranium and thorium) (Omeje et al., 2019; Wanjala et al., 2021).

In order to further understand whether there is significance difference between the data acquired in Amuloko and the data acquired in Olorunsogo, an independent sample test and an ANOVA test were performed on the acquired data at the two locations. A *t*-test is one of the inferential tests in statistics used to establish the difference that exist between means from two or more groups. Equations (4) and (5) are the relationships for estimating *t*-test (Gerald, 2018). The null hypothesis in this study is that there is no significant difference between the radon concentration sources in Amuloko groundwater and the radon concentration sources in Olorunsogo groundwater. The decision rule is that if the magnitude of the *t*-calculated value is greater than the *t*-critical value at significance level (α -value) of 0.05, the hypothesis is rejected (Machin et al., 2007). The independent samples test for the two locations is shown in Table 4. Based on the fact that the significance value (*p*-value) is greater than α -value, the equal variances assumed parameters are considered for the *t*-test. In Table 4, the *t*-critical (i.e. 2.024) is greater than the magnitude of the *t*-calculated. Therefore, the null hypothesis is accepted.

Table 3
Pearson’s correlation results of some variables in Amuloko and Olorunsogo groundwater.

Amuloko groundwater					Olorunsogo groundwater				
	Radon	Temp.	pH	Thoron		Radon	Temp.	pH	Thoron
Radon	1				Radon	1			
Temp.	-0.4266	1			Temp.	-0.3190	1		
pH	0.3114	-0.1328	1		pH	0.4104	0.2470	1	
Thoron	0.8949	-0.3833	0.2538	1	Thoron	0.5914	-0.0560	0.1860	1

Note: Radon and thoron units are in Bq L-1, Temp. ≡ Temperature unit is in °C.

Table 4
Independent samples test on radon concentrations in Amuloko and Olorunsogo groundwater.

	Levene’s test for EV			t-test for equality of \bar{x}							
	F	Sig. (p)	α	t _{cal.}	t _{cri.}	df	Sig. (2-tailed)	\bar{x} diff.	SE diff.	95% CI of the diff.	
										Lower	Upper
EVA	1.700	0.200	0.05	0.763	2.024	38.000	0.450	1.384	1.814	-2.288	5.056
EVNA				0.763	2.030	34.542	0.451	1.384	1.814	-2.300	5.068

Note: EVA=equal variances assumed, EVNA=equal variances not assumed, EV=equality of variances, \bar{x} = mean, F=F-ratio, Sig.=significance, p=p-value, α = α -value, t_{cal.}=t-calculated, t_{cri.}=t-critical, df=degree of freedom, diff.=difference, SE=standard error, CI=confidence interval.

$$t = \frac{\bar{x}_1 - \bar{x}_2}{Sp \sqrt{\frac{1}{n_1} + \frac{1}{n_2}}} \tag{4}$$

$$Sp = \sqrt{\frac{(n_2 - 1)S_1^2 + (n_2 - 1)S_2^2}{n_1 + n_2 - 2}} \tag{5}$$

where \bar{x}_1 and \bar{x}_2 are the first and the second sample means, n_1 and n_2 are the first and the second sample populations, S_1 and S_2 are the first and the second sample standard deviations, Sp is the pooled standard deviation.

An ANOVA test is a statistical measure to analyze the differences among population means. It is used to determine if the experimented results are significant or not (Kenton, 2021). In this study, a one-way ANOVA was used because only two groups (locations) are involved in the analysis. The ANOVA test can be determined by equation (6) (Sawyer, 2009). The ANOVA result for the two locations is shown in Table 5. The same hypothesis used for the t-test was established for the ANOVA. For variations to occur in the ANOVA result, F-ratio must be greater than 1 and p-value < α -value (Machin et al., 2007; Kenton, 2021). As shown in Table 5, F-ratio (0.582) \approx 1 and p-value (0.450) > α -value (0.05). This result further confirms that no variation exists between the source of radon concentrations in Amuloko shallow aquifers and that of Olorunsogo shallow aquifers.

$$F = \frac{MST}{MSE} \tag{6}$$

where F is the ANOVA coefficient, MST is the mean sum of squares due to treatment and MSE is the mean sum of squares due to noise. The MST indicates an indirect measure of differences in group mean, while MSE indicates the statistical noise or error since the variance is not explained by the effect of the independent variable on the dependent variable (Sawyer, 2009).

Table 5
The ANOVA test on radon concentrations in Amuloko and Olorunsogo groundwater.

	Sum of squares	df	Mean square	F	Sig. (p)
Between groups	19.157	1	19.157	0.582	0.450
Within groups	1250.004	38	32.895		
Total	1269.161	39			

Note: Same interpretation for Table 4.

Based on the descriptive statistics and the inferential tests (t-test and ANOVA) used in this study, high radon concentrations in groundwater towards the two fault planes at survey points 1 and 2 have been linked to the geological contributions of faults. This could have been due to iron oxidation during faulting and weathering of the parent rocks. Iron oxidation mostly results to exclusive iron-staining identity of fault zones and fractured rocks (Richey and Evans, 2013; Olorunfemi et al., 2020). This process increases the level of radon being emanated from fault planes through soils and rocks, which results to negative or low magnetic anomalies (that is, enhanced magnetic susceptibilities) (Olorunfemi et al., 2020) and high concentrations of radon in groundwater (Choubey and Ramola, 1997; Choubey et al., 2000; Al-Tamimi and Abumurad, 2001; Prasad et al., 2009, 2018). Furthermore, the major pathways of radon within fault zones are: dispersion and diffusion through permeable soils as a result of decayed ²³⁸U being accumulated in soils and upward migration of radon along faults and fractures through carrier gasses such as N₂ and CO₂ (Chen et al., 2018). Radon from the carrier gases are produced from both the decay of ²³⁸U at the crust-mantle interface and the one produced at the CaSiO₃ perovskite interface in the mantle (Wang et al., 2014; Zhou et al., 2015). Aquifers along the fault zones are contaminated with radon since one of the pathways for this gas to reach the surface due to its short half-life is through the fault plane. This is evident in the study of Oni et al. (2019b) where groundwater without storage tank had higher radon concentrations than the one with storage facilities.

This study agrees with the works of Choubey et al. (2000) at Himalayan springs and Asadi et al. (2015) near Anar fault in Iran. It was concluded in their studies that aquifers around the fault zone showed higher radon concentrations than those away from the fault zone. Furthermore, range of the (CRn)_w at the two locations in this study are compared with the results from other parts of the world as shown in Table 6. It was revealed that the maximum (CRn)_w obtained in all the locations as presented in Table 6 are above the global limit (GL) of 11.10 Bq l⁻¹, especially where the (CRn)_w obtained in the city of Zarand in Iran is greater than the GL by a factor of 1.30 and the (CRn)_w obtained in Shanomo and Bagwai areas in Kano, north-western Nigeria is greater than the GL by a factor of 4.50.

4. Conclusion

This study assessed the radon concentrations in groundwater sources and its health effects within shallow aquifers from two granitic terrains

Table 6
Comparison in the $(CRn)_w$ from this study and other locations.

Location	$(CRn)_w$ (Bq l ⁻¹)	$(AEDR)_{ing}$ (μSv y ⁻¹)	$(AEDR)_{inh}$ (μSv y ⁻¹)	$(AEDR)_{total}$ (μSv y ⁻¹)	Reference
Amuloko, Ibadan, southwestern Nigeria	3.00 to 24.50	21.90 to 178.85	7.56 to 61.74	29.46 to 240.59	This study
Olorunsogo, Ibadan, southwestern Nigeria	3.18 to 19.28	23.21 to 140.74	8.01 to 48.59	31.23 to 189.33	This study
Moro, northcentral Nigeria	16.75 to 19.18	122.28 to 140.01	42.21 to 48.33	164.49 to 188.35	Orosun et al. (2021)
Edu, northcentral Nigeria	21.58 to 27.93	157.53 to 203.89	54.38 to 70.38	211.92 to 274.27	Ajibola et al. (2021)
Kano, northwestern Nigeria	3.18 to 49.93	23.21 to 364.49	8.01 to 125.82	31.23 to 490.31	Bello et al. (2020)
Kaduna, northwestern Nigeria	13.90 to 22.40	101.47 to 163.52	35.03 to 56.45	136.50 to 219.97	Jibril et al. (2021)
Bauchi, northeastern Nigeria	4.92 to 46.25	35.92 to 337.63	12.40 to 116.55	48.31 to 454.18	Shu'aibu et al. (2022)
Zarand, Iran	4.67 to 31.55	34.09 to 230.32	11.77 to 79.51	45.86 to 309.82	Rahimi et al. (2022)
Anar city, Kerman Province, Iran	1.33 to 29.91	9.71 to 218.34	3.35 to 75.37	13.06 to 293.72	Asadi et al. (2016)
Zarand city and its Environs, Iran	5.16 to 14.40	37.67 to 105.12	13.00 to 36.29	50.67 to 141.41	Darabi et al. (2020)
Northern Rajasthan, India	0.50 to 22.00	3.65 to 160.60	1.26 to 55.44	4.91 to 216.04	Mittal et al. (2016)
Crete and Attica, Greece	0.80 to 24.00	5.84 to 175.20	2.02 to 60.48	7.86 to 235.68	Nikolopoulos and Louizi (2008)
Guaruja, Santos and Sao Vicente, Brazil	0.96 to 36.00	7.01 to 262.80	2.42 to 90.72	9.43 to 353.52	Marques et al. (2004)
Cyprus	0.30 to 20.00	2.19 to 146.00	0.76 to 50.40	2.95 to 196.40	Nikolopoulos and Louizi (2008)
Busan, South Korea	0.00 to 300.00	0.00 to 2190.00	0.00 to 756.00	0.00 to 2946.00	Cho et al. (2004)
Transylvania, Romania	0.50 to 129.30	3.65 to 943.89	1.26 to 325.84	4.91 to 1269.73	Cosma et al. (2008)
Erbil city, Iraq	4.00 to 12.18	29.20 to 88.91	10.08 to 30.69	39.28 to 119.61	Qadir et al. (2021)
Mosul city, Iraq	17.4 to 36.10	127.02 to 263.53	43.85 to 90.97	170.87 to 354.50	Qadir et al. (2021)
Southern Catalonia, Spain	1.40 to 105.00	10.22 to 766.50	3.53 to 264.60	13.75 to 1031.10	Fonollosa et al. (2016)
Canary Islands, Spain	0.30 to 76.90	2.19 to 561.37	0.76 to 193.79	2.95 to 755.16	Alonso et al. (2015)
Uttara Kannada district, India	2.37 to 171.35	17.30 to 1250.86	5.97 to 431.80	23.27 to 1682.66	Suresh et al. (2020)
Garhwal Himalaya, India	8.00 to 3050.00	58.40 to 22265.00	20.16 to 7686.00	78.56 to 29951.00	Prasad et al. (2008)
Maximum contamination limit	4.00 to 40.00	–	–	–	UNSCEAR (2006)
Global limit	11.10	100.00	NA	100.00	USEPA (1999) and UNSCEAR (2000)

in the south-eastern axis of Ibadan, Nigeria. Forty groundwater samples (in triplicates) were collected from the two settlements (Amuloko and Olorunsogo) being situated over granite gneiss in Ibadan. Geospatial variations in radon concentrations and the annual effective doses due to inhalation and ingestion for all the age groups (infants, children and adults) increased from the north-eastern axis to the south-western zone in Amuloko. Meanwhile, a reverse trend was observed in Olorunsogo. It was observed that the levels of radon concentrations in groundwater sources along the two fault zones are much higher than other locations (including the dumpsite and the river channel axis). The estimated means for the $(CRn)_w$ in Amuloko and in Olorunsogo area are higher than the global limit (GL) by factors of 1.21 and 1.09. The estimated means for the $(AEDR)_{total}$ by adults at the two locations are higher than the global limit (GL) by factors of 1.32 and 1.19. The AEDR received in water by all age groups from the two locations are in the order infants > children > adults. The AEDR received in water by all age groups indicated that no one is safe from the risks associated with consumption of radon-enriched water such as lung cancers, stomach cancers and other carcinogenic diseases that could affect the internal organs. The statistical analysis revealed that the radon pathway to the aquifer in the study locations is mainly through the geogenic contributions and anthropogenic source (such as dumpsite) has no effect on the radon concentrations. It is recommended that direct usage of groundwater without storage facilities that could minimize the level of radon in water (prior to treatments) at these settlements should be avoided.

Ethical approval

Not applicable.

Informed consent statement

Not applicable.

Funding

The data acquisition of this study was partially supported by the Covenant University Center for Research and Discovery's Grant (CUCRID/RC/02.04.21/VC).

Declaration of competing interest

The authors declare that they have no known competing financial interests or personal relationships that could have appeared to influence the work reported in this paper.

Data availability

Data will be made available on request.

Acknowledgment

The lead author thanks the management of the Covenant University for providing the Solar Powered Light and Electrical Supply System that was used during the data acquisition stage. The effort of all the reviewers of this article is greatly acknowledged.

References

- Abodunrin, O.P., Akinloye, M.K., 2020. Determination of radon exhalation rates from soil around buildings in Lagos environments using passive measurement technique. *J. Environ. Health Sci. Eng.* 18 (1), 129–135. <https://doi.org/10.1007/s40201-020-00446-3>.
- Adabanija, M.A., Afolabi, O.A., Lawal, L., 2020. The influence of bedrocks on groundwater chemistry in a crystalline basement complex of southwestern Nigeria. *Environ. Earth Sci.* 79, 87. <https://doi.org/10.1007/s12665-020-8822-y>.
- Adagunodo, T.A., 2017. Groundwater Pollution and Control: an Overview. (Chapter 1) in *Book: Groundwater Contamination: Performance, Limitations and Impacts*. Editor: Anna L Powell © 2017 Nova Science Publishers, Inc, pp. 1–135, 978-1-153611-017-3; 978-1-53611-003-6.
- Adagunodo, T.A., Akinloye, M.K., Sunmonu, L.A., Aizebeokhai, A.P., Oyeyemi, K.D., Abodunrin, F.O., 2018a. Groundwater exploration in aaba residential area of akure, Nigeria. *Front. Earth Sci.* 6, 66. <https://doi.org/10.3389/feart.2018.00066>.
- Adagunodo, T.A., Bayowa, O.G., Usikalu, M.R., Ojoawo, A.I., 2019a. MethodsX 6C. In: *Radiogenic Heat Production in the Coastal Plain Sands of Ipokia, Dahomey Basin, Nigeria*, pp. 1608–1616. <https://doi.org/10.1016/j.mex.2019.07.006>.
- Adagunodo, T.A., Lüning, S., Adeleke, A.M., Omidiora, J.O., Aizebeokhai, A.P., Oyeyemi, K.D., Hamed, O.S., 2018b. Evaluation of 0 ≤ M ≤ 8 Earthquake Data Sets in African-Asian Region during 1966 – 2015. <https://doi.org/10.1016/j.dib.2018.01.049>. Data in Brief 17C:588–603.
- Adagunodo, T.A., Sunmonu, L.A., Emeteri, M.E., 2018c. Heavy metals' data in soils for agricultural activities. *Data Brief* 18, 1847. <https://doi.org/10.1016/j.dib.2018.04.115>. –1855.
- Adagunodo, T.A., Sunmonu, L.A., Adabanija, M.A., Omeje, M., Odetunmbi, O.A., Ijeh, V., 2019b. Statistical assessment of radiation exposure risks to farmers in odo oba, southwestern Nigeria. *Bulletin of the Mineral Research and Exploration* 159, 201–217. <https://doi.org/10.19111/bulletinofmre.495321>.

- Adagunodo, T.A., Sunmonu, L.A., Oladejo, O.P., Olafisoye, E.R., 2013. Groundmagnetic investigation into the cause of the subsidence in the abandoned local government secretariat, Ogbomoso, Nigeria. *ARPN J. Earth Sci.* 2 (3), 101–109. http://www.arpnjournal.com/jes/research_papers/rp_2013/jes_0913_27.pdf.
- Ademola, J.A., Oyeleke, O.A., 2017. Radon-222 in groundwater and effective dose due to ingestion and inhalation in the city of Ibadan, Nigeria. *J. Radiol. Prot.* 37 (1), 189–200. <https://doi.org/10.1088/1361-6498/37/1/189>.
- Ahmed, M., Najemaldin, M., Abdulwhab, A., Ahmed, R., 2019. Estimation of Radon Gas Concentration in Soil and Drinking Water Supply Samples of Kirkuk Governorate, Iraq, vol. 6. *Journal of Garmian University*, pp. 26–33. <https://doi.org/10.24271/garmian.scpas4>. SCAPAS Conference).
- Airouche, R., Roudier, C., Clero, E., Ielsch, G., Gay, D., Guillevic, J., Marant, M.C., Vacquier, B., LeTertre, A., Laurier, D., 2018. Quantitative health impact of indoor radon in France. *Radiat. Environ. Biophys.* 57 (3), 205–214. <https://doi.org/10.1007/s00411-018-0741-x>.
- Ajibola, T.B., Orosun, M.M., Lawal, W.A., Akinyose, F.C., Salawu, N.B., 2021. Assessment of annual effective dose associated with radon in drinking water from gold and bismuth mining area of Edu, Kwara, north-central Nigeria. *Pollution* 7 (1), 231–240. <https://doi.org/10.22059/poll.2020.309470.892>.
- Aladejana, J.A., Odeyemi, O.O., Tijani, M.N., Hassan, I., 2018. Integrated assessment of leachate concentration in soil underlying Amuloko open waste dumpsite, Ibadan southwestern Nigeria. *J. Min. Geol.* 54 (1), 1–11.
- Ali, A.A., Abdullhussan, A.A., Asia, H.A., 2012. Radon and thoron concentration measurement of ground water in Kufa city by using RAD7 detector. *Journal of Kufa-Physics* 4 (2), 44–49.
- Ali, N., Khan, E.U., Akhter, P., Khan, F., Waheed, A., 2010. Estimation of mean annual effective dose through radon concentration in the water and indoor air of Islamabad and Murree. *Radiat. Protect. Dosim.* 141 (2), 183–191. <https://doi.org/10.1093/rpd/ncq160>.
- Alonso, H., Cruz-Fuentes, T., Rubiano, J.G., Gonzalez-Guerra, J., Cabrera, M.C., Arnedo, M.A., Tejera, A., Rodriguez-Gonzalez, A., Perez-Torrado, F.J., Martel, P., 2015. Radon in groundwater of the northeastern Gran Canaria aquifer. *Water* 7 (6), 2575–2590. <https://doi.org/10.3390/w7062575>.
- Al-Tamimi, M., Abumurad, K., 2001. Radon anomalies along faults in North of Jordan. *Radiat. Meas.* 34 (1–6), 397–400. [https://doi.org/10.1016/S1350-4487\(01\)00193-7](https://doi.org/10.1016/S1350-4487(01)00193-7).
- Asadi, M.A.A., Rahimi, M., Jabbari, K.L., 2016. The effect of geological structure on radon concentration dissolved in groundwater in nearby Anar fault based on a statistical analysis. *J. Radioanal. Nucl. Chem.* 308, 801–807. <https://doi.org/10.1007/s10967-015-4581-8>.
- Bello, S., Nasiru, R., Garba, N.N., Adeyemo, D.J., 2020. Annual effective dose associated with radon, gross alpha and gross beta radioactivity in drinking water from gold mining areas of Shanomo and Bagwai, Kano State, Nigeria. *Microchem. J.* 154, 104551. <https://doi.org/10.1016/j.microc.2019.104551>.
- Bem, H., Plota, U., Staniszevska, M., Bem, E.M., Mazurek, D., 2014. Radon (^{222}Rn) in underground drinking water supplies of the Southern Greater Poland Region. *J. Radioanal. Nucl. Chem.* 299 (3), 1307–1312. <https://doi.org/10.1007/s10967-013-2912-1>.
- Camacho, L.M., Gutiérrez, M., Alarcón-Herrera, M.T., Villalba, M. de L., Deng, S., 2011. Occurrence and treatment of arsenic in groundwater and soil in northern Mexico and southwestern USA. *Chemosphere* 83 (3), 211–225. <https://doi.org/10.1016/j.chemosphere.2010.12.067>.
- Chambers, S.D., Preunkert, S., Weller, R., Hong, S.B., Humphries, R.S., Tositti, L., Angot, H., Legrand, M., Williams, A.G., Griffiths, A.D., 2018. Characterizing atmospheric transport pathways to Antarctica and the remote southern ocean using radon-222. *Front. Earth Sci.* 6, 1–28.
- Chanyotha, S., Burnett, W.C., Taniguchi, M., Kritsanuwat, R., Sriplody, P., 2010. Experience in using radon and thoron data to solve environmental and water problems. *Radiat. Protect. Dosim.* 141 (4), 374–378. <https://doi.org/10.1093/rpd/ncq225>.
- Chen, Z., Li, Y., Liu, Z., Wang, J., Zhou, X., Du, J., 2018. Radon emission from soil gases in the active fault zones in the capital of China and its environmental effects. *Sci. Rep.* 8, 16772. <https://doi.org/10.1038/s41598-018-35262-1>.
- Cho, J.S., Ahn, J.K., Kim, H.-C., Lee, D.W., 2004. Radon concentrations in groundwater in Busan measured with a liquid scintillation counter method. *J. Environ. Radioact.* 75 (1), 105–112. <https://doi.org/10.1016/j.jenvrad.2003.06.002>.
- Choubey, V.M., Bartarya, S.K., Ramola, R.C., 2000. Radon in Himalayan springs: a hydrogeological control. *Environ. Geol.* 39 (6), 523–530. <https://doi.org/10.1007/s002540050463>.
- Choubey, V., Ramola, R., 1997. Correlation between geology and radon levels in groundwater, soil and indoor air in Bhilangana Valley, Garhwal Himalaya India. *Environ. Geol.* 32 (4), 258–262. <https://doi.org/10.1007/s002540050215>.
- Cosma, C., Moldovan, M., Dicu, T., Kovacs, T., 2008. Radon in water from transylvania (Romania). *Radiat. Meas.* 43 (8), 1423–1428. <https://doi.org/10.1016/j.radmeas.2008.05.001>.
- Darabi, F.Z., Rahimi, M., Malakootian, M., Javid, N., 2020. Studying radon concentration in drinking water resources in Zarand city (Iran) and its villages. *J. Radioanal. Nucl. Chem.* 326, 33–39. <https://doi.org/10.1007/s10967-020-07349-5>.
- Davies, T.C., 2010. *Medical Geology in Africa*. Medical Geology, pp. 199–219. https://doi.org/10.1007/978-90-481-3430-4_8.
- Duggal, V., Mehra, R., Rani, A., 2013. Analysis of radon concentration in drinking water in Hanumangarh district of Rajasthan, India. *Radiat. Protect. Environ.* 36 (2), 65. <https://doi.org/10.4103/0972-0464.128870>.
- DURRIDGE, 2013. *DURRIDGE Radon Instrumentation: Big Bottle RADH₂O User Manual*. DURRIDGE Company Inc., Billerica, USA.
- DURRIDGE, 2018a. *DURRIDGE Radon Capture and Analytics: Big Bottle System High Sensitivity Radon in Water Accessory for the RAD7 with Aerator Cap Revision B User Manual*. DURRIDGE Company Inc., USA. Technology Park Drive, Billerica, MA 01821. <https://durridge.com/documentation/Big%20Bottle%20System%20Manual%20Aerator%20Cap%20Rev%20B.pdf>.
- DURRIDGE, 2018b. *DURRIDGE Radon Capture and Analytics*. <https://durridge.com/documentation/RAD7%20Specifications.pdf>.
- Esan, D.T., Sridhar, M.K.C., Obed, R., Ajiboye, Y., Afolabi, O., Olubodun, B., Oni, O.M., 2020. Determination of residential soil gas radon risk indices over the lithological units of a southwestern Nigeria university. *Sci. Rep.* 10 (1), 7368. <https://doi.org/10.1038/s41598-020-64217-8>.
- Ezzulddin, S.K., Mansour, H.H., 2017. Assessment of radon exposure in Erbil drinking water resources. *ZANCO Journal of Pure and Applied Sciences* 29 (4), 184–194. <https://doi.org/10.21271/ZJPAS.29.s4.22>.
- Ferreira, A.O., Pecequilo, B.R.S., Aquino, R.R., 2011. Application of a “sealed can technique” and CR-39 detectors for measuring radon emanation from undamaged granitic ornamental building materials. *Radioprotection* 46 (6), S49–S54. <https://doi.org/10.1051/radiopro/20116557s>.
- Finne, I.E., Kolstad, T., Larsson, M., Olsen, B., Prendergast, J., Rudjord, A.L., 2019. Significant reduction in indoor radon in newly built houses. *J. Environ. Radioact.* 196, 259–263. <https://doi.org/10.1016/j.jenvrad.2018.01.013>.
- Fonollosa, E., Penalver, A., Borrull, F., Aguilar, C., 2016. Radon in spring waters in the south of Catalonia. *J. Environ. Radioact.* 151, 275–281. <https://doi.org/10.1016/j.jenvrad.2015.10.019>.
- Ganiyu, S.A., Badmus, B.S., Olurin, O.T., Ojekunle, Z.O., 2018. Evaluation of seasonal variation of water quality using multivariate statistical analysis and irrigation parameter indices in Ajakanga area, Ibadan, Nigeria. *Appl. Water Sci.* 8, 35. <https://doi.org/10.1007/s13201-018-0677-y>.
- Gaskin, J., Coyle, D., Whyte, J., Krewski, D., 2018. Global estimate of lung cancer mortality attributable to residential radon. *Environ. Health Perspect.* 126 (5), 057009. <https://doi.org/10.1289/EHP2503>.
- Gerald, B., 2018. A brief review of independent, dependent and one sample t-test. *International Journal of Applied Mathematics and Theoretical Physics* 4 (2), 50–54. <https://doi.org/10.11648/j.ijamtp.20180402.13>.
- Ghias, S., Satti, K.H., Khan, M., Dilband, M., Naseem, A., Jabbar, A., Kali, S., Ur-Rehman, T., Nawab, J., Aqeel, M., Khan, M.A., Zafar, M.I., 2021. Health risk assessment of radioactive footprints of the urban soils in the residents of dera ghazi khan, Pakistan. *Chemosphere* 267, 129171. <https://doi.org/10.1016/j.chemosphere.2020.129171>.
- Groeneveld, R.A., Meeden, G., 1984. Measuring skewness and kurtosis. *The statistician* 33 (4), 391–399. <https://doi.org/10.2307/2987742>.
- Grundy, A., Brand, K., Khandwala, F., Poirier, A., Tamminen, S., Friedenreich, C.M., Brenner, D.R., 2017. Lung cancer incidence attributable to residential radon exposure in Alberta in 2012. *CMAJ Open* 5 (2), E529–E534. <https://doi.org/10.9778/cmajo.20160053>.
- Health Canada, 2018. *Radon: is it in your home?*. In: *Information for Health Professionals*. Health Canada, Canada, 978-0-660-25828-7.
- Hopke, P.K., Borak, T.B., Doull, J., Cleaver, J.E., Eckerman, K.F., Gundersen, L.C.S., Harley, N.H., Hess, C.T., Kinner, N.E., Kopecky, K.J., McKone, T.E., Sextro, R.G., Simon, S.L., 2000. Health risks due to radon in drinking water. *Environ. Sci. Technol.* 34 (6), 921–926. <https://doi.org/10.1021/es9904134>.
- Howard, G., Bartram, J., 2003. *Domestic Water Quality, Service Level and Health*. WHO, Geneva (Switzerland).
- Hwa, O.Y., Kim, G., 2015. A radon-thoron isotope pair as a reliable earthquake precursor. *Sci. Rep.* 5, 13084. <https://doi.org/10.1038/srep13084>.
- ICRP (International Commission on Radiological Protection), 2009. *International Commission on Radiological Protection Ref 00/902/09, Statement on Radon*. ICRP ref 00/902/09.
- Igarashi, G., Saeki, S., Takahata, N., Sumikawa, K., Tasaka, S., Sasaki, Y., Takahashi, M., Sano, Y., 1995. Ground-water radon anomaly before the kobe earthquake in Japan. *Science* 269, 60–61. <https://doi.org/10.1126/science.269.5220.60>.
- Jibril, M.K., Garba, N.N., Nasiru, R., Ibrahim, N., 2021. Assessment of radon concentrations in water sources from Sabon Gari local government area, Kaduna State, Nigeria. *FUDMA Journal of Sciences* 5 (1), 254–260. <https://doi.org/10.33003/fjs-2021-0501-563>.
- Kenton, W., 2021. *Analysis of Variance (ANOVA). Fundamental Analysis, Tools for Fundamental Analysis*. Investopedia. Retrieved on November 16, 2021. <https://www.investopedia.com/terms/a/anova.asp>.
- Khan, F., 2011. In: D Thesis, N.W.F.P. Ph (Ed.), *Measurement of Radon Concentration in Water, Soil and Air in and Around Earthquake Hit Areas*. Department of Physics, COMSATS Institute of Information Technology, Islamabad, Pakistan.
- Lane-Smith, D., Schubert, M., 2020. Absolute measurement of thoron in surface waters. *Water* 12, 3083. <https://doi.org/10.3390/w12113083>.
- Lapworth, D.J., Nkhuwa, D.C.W., Okotto-Okotto, J., Pedley, S., Stuart, M.E., Tijani, M.N., Wright, J., 2017. Urban groundwater quality in sub-saharan Africa: current status and implications for water security and public health. *Hydrogeol. J.* 25 (4), 1093–1116. <https://doi.org/10.1007/s10040-016-1516-6>.
- Lawrence, C.E., Akber, R.A., Bollhöfer, A., Martin, P., 2009. Radon-222 exhalation from open ground on and around a uranium mine in the wet-dry tropics. *J. Environ. Radioact.* 100, 1–8.
- Machin, D., Campbell, M.J., Walters, S.J., 2007. *Medical Statistics: a Textbook for the Health Sciences*, fourth ed. John Wiley and Sons, Ltd. The Atrium, Southern Gate, Chichester, West Sussex PO19 8SQ, England, ISBN 978-0-470-02519-2.
- Marques, A.L., Santos, W.D., Geraldo, L.P., 2004. Direct measurement of radon activity in water from various natural sources using nuclear track detectors. *Appl. Radiat. Isot.* 60, 801–804. <https://doi.org/10.1016/j.apradiso.2004.01.015>.

- Mittal, S., Rani, A., Mehra, R., 2016. Estimation of radon concentration in soil and groundwater samples of northern Rajasthan, India. *Journal of Radiation Research and Applied Sciences* 9, 125–130. <https://doi.org/10.1016/j.jrras.2015.10.006>.
- Modibo, O.B., Tamakuma, Y., Suzuki, T., Yamada, R., Zhuo, W., Kranrod, C., Iwaka, K., Akata, N., Hosoda, M., Tokonami, S., 2021. Long-term measurements of radon and thoron exhalation rates from the ground using the vertical distributions of their activity concentrations. *Int. J. Environ. Res. Publ. Health* 18, 1489. <https://doi.org/10.3390/ijerph18041489>.
- Narayana, Y., Rajashekara, K.M., Siddappa, K., 2007. Natural radioactivity in some major rivers of coastal Karnataka on the southwest coast of India. *J. Environ. Radioact.* 95 (2–3), 98–106. <https://doi.org/10.1016/j.jenvrad.2007.02.003>.
- Nasir, T., Shah, M., 2012. Measurement of annual effective doses of radon from drinking water and dwellings by CR-39 Track detectors in Kulachi city of Pakistan. *J. Basic Appl. Sci.* 8, 528–536. <https://doi.org/10.6000/1927-5129.2012.08.02.44>.
- Nikolopoulos, D., Louizi, A., 2008. Study of indoor radon and radon in drinking water in Greece and Cyprus: implications to exposure and dose. *Radiat. Meas.* 43, 1305–1314. <https://doi.org/10.1016/j.radmeas.2008.03.043>.
- Normality Testing, 2019. Normality Testing, Skewness and Kurtosis. Retrieved on November 11, 2021. <https://help.gooddata.com/doc/en/reporting-and-dashboards/maql-analytical-query-language/maql-expression-reference/aggregation-functions/statistical-functions/predictive-statistical-use-cases/normality-testing-skewness-and-kurtosis>.
- Okunlola, A.O., Adeigbe, O.C., Oluwatoko, O.O., 2009. Compositional and petrogenetic features of schistose rocks of Ibadan area, southwestern Nigeria. *Earth Sci. Res. J.* 13, 29–43.
- Oladapo, O.O., Adagunodo, T.A., Aremu, A.A., Oni, O.M., Adewoye, A.O., 2022. Evaluation of soil-gas radon concentrations from different geological units with varying strata in a crystalline basement complex of southwestern Nigeria. *Environ. Monit. Assess.* 194, 486. <https://doi.org/10.1007/s10661-022-10173-x>.
- Oladejo, O.P., Adagunodo, T.A., Sunmonu, L.A., Adabanija, M.A., Olasunkanmi, N.K., Omeje, M., Babarimisa, I.O., Bility, H., 2019. Structural analysis of subsurface stability using aeromagnetic data: a case of Ibadan, southwestern Nigeria. *IOP Conf Series: J. Phys. Conf.* 1299, 012083 <https://doi.org/10.1088/1742-6596/1299/1/012083>.
- Olafisoye, E.R., Sunmonu, L.A., Ojoawo, A., Adagunodo, T.A., Oladejo, O.P., 2012. Application of very low frequency electromagnetic and hydro-physicochemical methods in the investigation of groundwater contamination at aarada waste disposal site, Ogbomoso, southwestern Nigeria. *Australian Journal of Basic and Applied Sciences* 6 (8), 401–409.
- Olorunfemi, M.O., Oni, A.G., Bamidele, O.E., Fadare, T.K., Aniko, O.O., 2020. Combined geophysical investigations of the characteristics of a regional fault zone for groundwater development in a basement complex terrain of south-west Nigeria. *SN Appl. Sci.* 2, 1033. <https://doi.org/10.1007/s42452-020-2363-6>.
- Omeje, M., Adagunodo, T.A., Akinwumi, S.A., Adewoyin, O.O., Joel, E.S., Husin, W., Mohd, S.H., 2019. Investigation of driller's exposure to natural radioactivity and its radiological risks in low latitude region using neutron activation analysis. *Int. J. Mech. Eng. Technol.* 10 (1), 1897–1920.
- Omosehinmi, D.E., Arogunjo, A.M., 2016. Geostatistical investigation and ambient radiation mapping of Akure north and south local government areas of Ondo state, Nigeria. *International Journal of Scientific Development and Research* 1 (12), 122–136.
- Oni, E.A., Adagunodo, T.A., 2019. Assessment of radon concentration in groundwater within Ogbomoso, SW Nigeria. *IOP Conf Series: J. Phys. Conf.* 1299, 012098 <https://doi.org/10.1088/1742-6596/1299/1/012098>.
- Oni, E.A., Adagunodo, T.A., Adegbite, A.A., Omeje, M., 2021. Determination of radon gas in bottled and sachet water in ile-ife, Nigeria. *IOP Conf. Ser. Earth Environ. Sci.* 655, 012092 <https://doi.org/10.1088/1755-1315/655/1/012092>.
- Oni, O.M., Amoo, P.A., Aremu, A.A., 2019b. Simulation of absorbed dose to human organs and tissues associated with radon in groundwater use in southwestern Nigeria. *Radiat. Phys. Chem.* 155, 44–47. <https://doi.org/10.1016/j.radphyschem.2018.08.029>.
- Oni, O.M., Yusuff, I.M., Adagunodo, T.A., 2019a. Measurement of radon-222 concentration in soil-gas of Ogbomoso southwestern Nigeria using RAD7. *Int. J. History Sci. Studies Res.* 1 (3), 1–8.
- Orosun, M.M., Ajibola, T.B., Akinyose, F.C., Osanyinlusi, O., Afolayan, O.D., Mahmud, M.O., 2021. Assessment of ambient gamma radiation dose and annual effective dose associated with radon in drinking water from gold and lead mining area of Moro, North-Central Nigeria. *J. Radioanal. Nucl. Chem.* 328 (1), 129–136. <https://doi.org/10.1007/s10967-021-07644-9>.
- Orosun, M.M., Usikal, M.R., Oyewumi, K.J., Adagunodo, T.A., 2019. Natural radionuclides and radiological risk assessment of granite mining field in asa, north-central Nigeria. *MethodsX* 6, 2504–2514. <https://doi.org/10.1016/j.mex.2019.10.032>.
- Oruncak, B., Ozkan, D., 2020. Variation of radon-radium gas in geothermal region of Omer-Gecek. *Arabian J. Geosci.* 13, 646. <https://doi.org/10.1007/s12517-020-05674-3>.
- Prasad, M., Kumar, G.A., Sahoo, B.K., Ramola, R.C., 2018. A comprehensive study of radon levels and associated radiation doses in Himalayan groundwater. *Acta Geophys.* 66, 1223–1231. <https://doi.org/10.1007/s11600-018-0135-0>.
- Prasad, Y., Prasad, G., Choubey, V.M., Ramola, R.C., 2009. Geohydrological control on radon availability in groundwater. *Radiat. Meas.* 44 (1), 122–126. <https://doi.org/10.1016/j.radmeas.2008.10.006>.
- Prasad, G., Prasad, Y., Gustain, G.S., Ramola, R.C., 2008. Measurement of radon and thoron levels in soil, water and indoor atmosphere of Budhakedar in Garhwal Himalaya, India. *Radiat. Meas.* 43, S375–S379. <https://doi.org/10.1016/j.radmeas.2008.04.050>.
- Qadir, R.W., Asaad, N., Qadir, K.W., Ahmad, S.T., Abdullah, H.Y., 2021. Relationship between radon concentration and physicochemical parameters in groundwater of Erbil City, Iraq. *Journal of Radiation Research and Applied Sciences* 14 (1), 61–69. <https://doi.org/10.1080/16878507.2020.1856588>.
- Rahimi, M., Asadi, A.M.M., Koopaei, L.J., 2022. Radon concentration in groundwater, its relation with geological structure and some physicochemical parameters of Zaranid in Iran. *Appl. Radiat. Isot.* 185, 110223 <https://doi.org/10.1016/j.apradiso.2022.110223>.
- Raji, W.O., 2014. Review of electrical and gravity methods of near-surface exploration for groundwater. *Niger. J. Technol. Dev.* 11 (2), 31–38.
- Richey, D.J., Evans, J.P., 2013. Fault architecture, linkage and internal structure: field examples from the iron wash fault zone, central Utah. *Gulf Coast Association of Geological Society* 42, 91–112.
- Saad, A.M., Sakr, M.A.H., Omar, A.E., Tamsah, Y.A., 2020. Assessment of radioactivity and geotechnical characteristics of soil foundation for suitability of safe urban extension using geospatial technology near Sahl Hasheedh Marin Port, eastern desert, Egypt. *Int. J. Environ. Anal. Chem.* 1–23. <https://doi.org/10.1080/03067319.2020.1802444>.
- Saç, M.M., Ortubuk, F., Kumru, M.N., İçhedef, M., Sert, Ş., 2012. Determination of radioactivity and heavy metals of Bakırçay river in Western Turkey. *Appl. Radiat. Isot.* 70 (10), 2494–2499. <https://doi.org/10.1016/j.apradiso.2012.06.019>.
- Saeed, S.H., Hassan, S.Y., 2015. Determination of radon, uranium and other radioactive isotopes' concentration in different types of natural water in nenava governorate. *Jordan Journal of Physics* 8 (4), 227–244.
- Sakr, M.A.H., Saad, A.M., Omar, A.E., Elkholi, S.M., El Shafae, O., 2022. Geospatial technology utilization for geotechnical hazard evaluation of sustainable urban development of Buraydah City, Kingdom of Saudi Arabia. *Arabian J. Geosci.* 15, 1320. <https://doi.org/10.1007/s12517-022-10546-z>.
- Sawyer, S.F., 2009. Analysis of variance: the fundamental concepts. *J. Man. Manip. Ther.* 17 (2), 27E–38E. <https://doi.org/10.1179/jmt.2009.17.2.27E>.
- Sustainable Development Goals, S.D.G., 2019. The Human Rights Guide to the Sustainable Development Goals: Goals, Targets and Indicators. The Danish Institute for Human Rights. Wilders Plads 8K, 1403 Copenhagen K, Denmark. <https://sdg.humanrights.dk/en/goals-and-targets>. Retrieved on August 18, 2022.
- Sharma, N., Singh, J., Esakki, S.C., Tripathi, R.M., 2016. A study of the natural radioactivity and radon exhalation rate in some cement used in India and its radiological significance. *J. Radiation Res. Appl. Sci.* 9, 47–56.
- Shu'aibu, H.K., Khandaker, M.U., Baballe, A., Tata, S., Adamu, M.A., 2021. Determination of radon concentration in groundwater of Gadau, Bauchi State, Nigeria and estimation of effective dose. *Radiat. Phys. Chem.* 178, 108934 <https://doi.org/10.1016/j.radphyschem.2020.108934>.
- Sukanya, S., Noble, J., Joseph, S., 2022. Application of radon (²²²Rn) as an environmental tracer in hydrogeological and geological investigations: an overview. *Chemosphere* 303, 135141. <https://doi.org/10.1016/j.chemosphere.2022.135141>.
- Sunmonu, L.A., Adagunodo, T.A., Olafisoye, E.R., Oladejo, O.P., 2012. The groundwater potential evaluation at industrial estate Ogbomoso southwestern Nigeria. *RMZ Mater. Geoenviron* 59 (4), 363–390.
- Suresh, S., Rangaswamy, D.R., Srinivasa, E., Sannappa, J., 2020. Measurement of radon concentration in drinking water and natural radioactivity in soil and their radiological hazards. *J. Radia. Res. Applied Sci.* 13 (1), 12–26. <https://doi.org/10.1080/16878507.2019.1693175>.
- Surfer Version, 2021. Surfer Mapping System. Golden Software, Inc., Golden, Colorado, USA.
- Tanner, A.B., 1964. Radon mitigation in the ground: a review. In: Adams, J.A.S., Lowder, W.M. (Eds.), *The Natural Radiation Environment*. University of Chicago Press, pp. 161–191.
- UNSCEAR, 2000. Sources, effects and risks of ionization radiation. In: Report to the General Assembly, with Scientific Annexes B: Exposures from Natural Radiation Sources. United Nations Scientific Committee on the Effects of Atomic Radiation, New York, USA.
- UNSCEAR (The United Nations Scientific Committee on the Effects of Atomic Radiation), 2006. Report to the General Assembly, Vol 1: Effects of Ionizing Radiation with Scientific Annexes A and B.
- USEPA, 1999. Radon in Drinking Water: Health Risk Reduction and Cost Analysis, vol. 64. Federal Register, Washington, USA.
- Usikal, M.R., Onumojor, C.A., Achuka, J.A., Akinpelu, A., Omeje, M., Adagunodo, T.A., 2020. Monitoring of radon concentration for different building types in covenant university, Nigeria. *Cogent Engineering* 7, 1759396. <https://doi.org/10.1080/23311916.2020.1759396>.
- Wanjala, F.O., Hashim, N.O., Otswana, D., Kebwaro, J., Chege, M., Nyambura, C., Carmen, A., 2021. Lung cancer risk assessment due to radon and thoron exposure in dwellings in Ortum, Kenya. *J. Environ. Poll. Human Health* 9 (2), 64–70. <https://doi.org/10.12691/jephh-9-2-5>.
- Wang, Y.J., Wu, T.L., Zhou, D.M., Chen, M.H., 2017. Advances in soil heavy metal pollution evaluation based on bibliometrics analysis. *J. Agro-Environ. Sci.* 6 (12), 2365–2378.
- Wang, X., Li, Y., Du, J., Zhou, X., 2014. Correlations between radon in soil gas and the activity of seismogenic faults in the Tangshan area, North China. *Radiat. Meas.* 60 (1), 8–14. <https://doi.org/10.1016/j.radmeas.2013.11.001>.
- Who, 2004. Guidelines for Drinking-Water Quality: Volume 1: Recommendations third ed. WHO, Geneva.
- Who, 2011. Guidelines for Drinking Water Quality, fourth ed. World Health Organization, Geneva (Chapter 9): Radiological Aspect? Switzerland.
- WHO (World Health Organization), 2018. World Health Organization Latest Global Cancer Data: Cancer Burdens Rises to 18.1 Million New Cases and 9.8 Million Cancer

- Deaths in 2018, September 12. World Health Organization, Geneva, Switzerland, p. 2018.
- WHO (World Health Organization), 2009. WHO Handbook on Indoor Radon: A Public Health Perspective. WHO, Geneva, Switzerland.
- Wu, Y., Hung, M., 2016. Comparison of spatial interpolation techniques using visualization and quantitative assessment. *Appl. Spatial Stat.* Ming-Chih Huh. <https://doi.org/10.5772/65996>. Available at: <https://www.intechopen/chapters/52704>.
- Yusuff, I.M., Adagunodo, T.A., Omoloye, M.A., Olanrewaju, A.M., 2019. Interdependency of soil-gas radon-222 concentration on soil porosity at different soil-depths. *IOP Conf Series: J. Phys. Conf.* 1299, 012099 <https://doi.org/10.1088/1742-6596/1299/1/012099>.
- Zhang, Y., Lu, L., Chen, C., Field, R.W., D'Alton, M., Kahe, K., 2022. Does protracted radon exposure play a role in the development of dementia? *Environ. Res.* 210, 112980 <https://doi.org/10.1016/j.envres.2022.112980>.
- Zhou, X., Chen, Z., Cui, Y., 2015. Environmental impact of CO₂, Rn, Hg degassing from the rupture zones produced by Wenchuan. MS 8.0 earthquake in western Sichuan, China. *Environ. Geochem. Health* 38 (5), 1067–1082. <https://doi.org/10.1007/s10653-015-9773-1>.